OVERVIEW OF STUDIES CONDUCTED IN FRANCE TO ASSESS THE BENEFIT OF A SPACE BASED BACKSCATTER LIDAR FOR A RADIATION AND CLIMATE WATCH MISSION

Pierre H. Flamant [1] and Jacques Pelon [2]

[1] *Laboratoire de Météorologie Dynamique du CNRS*
[2] *Service d'Aéronomie du CNRS*

1. INTRODUCTION

The growing interest world wide in climate change and climate variability prompted new studies to answer the concerns raised during the past decades. The cloud-radiation interaction is a key feature of the climat system linking the incoming solar radiation to atmospheric dynamics and surface processes. The studies adress simultaneously 1) a better description of the various components and complex processes taking place in the global climat system and 2) advanced modelings with their relevant parametrizations, at global or regional scales. Going along with these goals a renew of interest was given to instrumental problems and their adequacy to tackle the objectives presented above. A special attention was drawn to remote sensors with airborne capability and great potential for future space applications. In this context the backscatter lidar technique has proven a powerful tool for the retrieval of clouds and aerosols properties. At the present, the applications cover the use of a single ground based lidar in synergy with others sensors, lidar networking like the international ECLIPS project [Platt et al., 1994], airborne projects and more recently the NASA LITE project on the shuttle Discovery. In the frame work of international activities, the relevant french activities and european activities in climat research involving lidar are presented in the next section.

2. LIDAR ACTIVITIES RELEVANT TO CLIMATE RESEARCH

The french scientific community expressed a strong interest in studies devoted to climate change, and participates actively to international and european programs. In this frame work two CNRS laboratories namely Laboratoire de Météorologie Dynamique (LMD) and Service d'Aéronomie (SA) developed ground-based lidars and an airborne backscatter lidar so-called LEANDRE-1 [Pelon et al., 1990]. This airborne lidar can look at zenith and nadir during the same flight, it takes about one minute to switch the pointing configuration. It uses a Nd-YAG transmitter making measurements at 0.53 and 1.06 μm simultaneously, with depolarization diversity at 0.53 μm.

Since 1989 LMD and SA participate to several major field campaigns dedicated to cloud-radiation interaction and radiative budget of the atmosphere : ICE in 1989 [Ansmann et al., 1993], ELAC in 1990 [Flamant and Pelon, 1992], ECLIPS II in 1991 [Valentin et al., 1993], ASTEX in 1992 [Weill et al., 1996], CIRREX in 1993 [Elouragini et al., 1996], and more recently in 1994 EUCREX [Brogniez et al., 1995], ECLIPS III and E-LITE [Flamant et al., 1995, Pelon et al, 1995/1]. The field campaigns were supported by french agencies : CNRS and CNES, and the European Space Agency and European Community.

In the area of airborne activities there exist three on-going major french projects as follow on of LEANDRE-1. They are : 1) a DIAL lidar (LEANDRE-2) for water vapor measurement, the validation flights have been conducted in September 1995, 2) the franco-german wind Doppler lidar so-called WIND developed jointly by CNRS-CNES and DLR-Munich, the technical flights are foreseen in early 1998, 3) a radar-lidar payload for cloud-dynamics interaction studies, it is under development jointly by CNRS-CNES and GKSS-Hamburg.

Regarding the application of the lidar technique in space, CNES conducted a preliminary study so-called BEST in the mid 80's aiming at a definition for a multiple instruments payload combining active et passive remote sensors : radar, lidars, microwave profiler, and visible and infrared imager. The objective of the mission was focused on the energy budget of the tropics for it is a key component of the global climate system. A DIAL lidar pointing at nadir and a quadbeam Doppler lidar were studied as core instruments in the frame work of the BEST to

provide with clouds and aerosols features, water vapor and wind profiles in the depth of the lower atmosphere. The study on wind Doppler lidar stressed a concept of multiple fixed line of sight to overcome several technical problems. At the present, scientists from CNRS laboratories are currenty involved in on-going activities at the European Space Agency. Presently, these studies considere a backscatter lidar and a wind Doppler lidar so-called ATLID and ALADIN respectively, and the definition of a "Radiation Mission" and an "Atmospheric Dynamic Mission" for the years 2000. They considere both free flyer or the International Space Station for the missions.
In the frame work of airborne and space based projects the CNRS laboratories developed various simulation tools i.e. advanced instrumental simulators for backscatter, DIAL and wind Doppler lidars. They have been used to assess the performances and sampling capabilities. Refarding the space application mythical lidars are flown in numerical model for large scale cloudiness built using either the ISCCP data base or General Circulation Model outputs.
Now, restricting the discussion to backscatter lidar and their application to global climate research, section 3 presents the objectives for observations from space and the relevant studies to be conducted. The retrieval of large scale cloudiness by a space based lidar is adressed in section 4. In section 5 the cloudiness variability at the meso scale is discussed and illustrated with examples from field campaigns. Section 6 presents the synergism between an airborne backscatter lidar and infrared radiometers and/or visible-near infrared imagers.

3. OBJECTIVES AND RELEVANT STUDIES

Considering a mission lasting 3 years in space for climate research, the scientific objectives for a backscatter lidar are :

- monitoring of the environment, aerosols transport and aerosols processing by clouds ;
- radiative transfer in the atmosphere and cloud-radiation interaction ;
- radiation-dynamics interaction.

The parameters of interest for process dedicated studies and sub grid parametrization in GCM and regional models are :

- large scale cloudiness, spatial distribution of stratiform clouds versus convective clouds, distribution of homogeneous clouds versus broken cloud fields, identification of multilayer clouds ;
- cloud radiative parameters, 3D-structure, optical properties, ice/water discrimination, microphysical parameters (liquide water content, effective radius of scatterers) ;
- aerosols layers, their structure and spatial distribution, optical parameters, and discrimination between aerosols layers and clouds,
- planetary boundary layer height.

To fulfill the objectives given above various studies have to be conducted to assess the benefit of a backscatter lidar in space. Proceeding from the large scale to smaller scale they are :

- retrieval of cloudiness at the large scale, and comparison with the ISCCP data base ;
- cloud variability at meso-scale and smaller scales relevant to both a sampling strategy from space and model resolution ;
- lidar signal inversion method adressing the lidar ambiguity with respect to backscatter-to-extinction lidar ratio, and multiple scattering processes.

Only the two first items are adressed in the two following sections 4 and 5. Another aspect is the synergy with passive remote sensors, it is presented in section 6.

4. RETRIEVAL OF CLOUDINESS AT LARGE SCALE

A space borne backscatter lidar is foresseen to retrieve cloud and aerosols layers structure and their radiative parameters, and the planetary boundary layer height at the global scale. An assessment of the performance on a single shot has been conducted using an instrument simulator. It relies on signal to noise ratio and cloud or aerosols optical properties. In turn the SNR depends on daytime or nighttime condition, orbit height and instrument parameters, i.e. equivalent transmitted laser energy per pulse and telescope collecting area. Both the 1.06 μm and 0.53 μm wavelengths transmitted by a Nd-YAG laser are considered in the ATLID project. The cloud altitude can be determined in a straight forward manner from lidar signal. Both the top and base altitudes can be determined for semi transparent clouds like cirrus provided the optical depth does not exceed about 2. It may require an averaging over tens of lidar shots or

more depending on the laser transmitted energy and cirrus optical depth. The top for dense clouds is currently detected on a single shot or by averaging a few shots. The detection of multilayer clouds is possible as illustrated by the results from LITE. It is due to the combinaison of a small lidar beam and small scale optical porosity or fractional cloudiness, and occurrence of multiple scattering in dense cloud layers. A multiple scattering effect does good and bad at the same time, it is beneficial to vertical sounding range capability, but it is detrimental to an accurate measurements of optical properties. The discrimination between ice and liquid water relies on a polarisation diversity capability for the instrument. It can be implemented for a space based backscatter lidar but it requires a carefull analysis to discriminate from multiple scattering.

In order to assess the capability for a space based lidar to retrieve large scale cloudiness a comparison have been conducted between a mythical lidar with cross track scanning (± 23°) and passive radiometer with improved ISCCP inversion algorithm [Pelon et al., 1995/2]. The comparison was conducted using the LMD General Circulation Model. The grid mesh is 64 points in longitude and 50 points in latitude, the cloudiness is broken down among 11 levels from the surface up to 15 km. Both a maximal and random overlaps between cloud layers are considered in the simulations. Prior a full simulation it has been determined that an optical depth of 0.3 for cirrus is significante for radiation transfer, it corresponds to a ±10 W m^{-2} variation in net flux at the top of the atmosphere (+) and surface (-).

An example of the results is displayed on Figure 1. It shows the cloudiness (inpercentage) for cirrus at 9.8 km built by the LMD GCM (panel a) to be used as an imput for the simulation exercice, and the cloudiness retrieved by a backscatter lidar orbiting the earth (panel b). The results show that using SNR ≥ 4 at cloud top thin cirrus with optical depth larger than 0.1/0.2 are detected with a 80 % reliability, while it is 50 % for ISCCP following the same exercice. Accordingly a significant improvement is expected in cirrus climatology with a space based lidar. The results show as well that multilayer cloud structures are well retrieved by lidar. This conclusion adress the importance of large scale cloudiness climatology to validate the physics and parametrizations used in GCM. For the retrieval of surface fluxes, it has been shown that the planetary boundary layer height is retrieved by averaging over a large number of lidar shots corresponding to 150x150 km^2 areas.

5. MESO-SCALE VARIABILITY

The meso scale and small scale variabilities of cloud properties adress the representativity of lidar measurements for the foot print is small, especially on a single shot basis as it stands for dense clouds. The variability of any cloud property can be represented by a histogram displaying this parameter as a function of occurence. Hereafter the studies refere to mid-latitude clouds and the results obtained during the field campaigns presented in section 2. The optical parameters are derived at 0.53 μm.

Cirrus. Histograms drawn for cirrus show two main types of behavior for the statistical distributions according to the cirrus optical depth. For low optical depth it is nearly exponential negative while the distribution for the geometrical thickness is nearly gaussian (figure 2). Accordingly there is no clear correlation between the two parameters. For thick cirrus the spatial distribution is more homogeneous and the distributions are gaussian for both the optical depth and geometrical thickness (figure 3). Then the correlation between the two parameters is good, it defines a limited area i.e. a mean point with the two standard deviations along the respective axis. In general, a cirrus can display the two features at the mesoscale, it results in two modes statistical distributions. This results have been obtained during ECLIPS III in 1994 (see section 2). The same distributions have been obtained during EUCREX'94 using the airborne lidar LEANDRE-1.

A one year lidar monitoring as been undertaken at LMD (48°N, 02°E) during CIRREX'93 [Elouragini et al., 1996]. The observations were made when only cirrus were present with no other clouds. The time series of lidar measurements on a day-by-day basis last from less than one hour to several hours. The statistical parameters are presented in Table 1.

Dense low clouds. The statistical properties of low dense clouds can be studied using histrograms as well. For the cloud top can be detected on a single shot basis the statistical distribution adresses directly the representativity of a single measurement from space. As an

example, the distribution (solid line) of the top altitude of marine stratocumulus over a distance of 36 km is displayed on figure 4. A gaussian shape distribution (dashed line) is plotted for comparison using the same standard deviation. They are in good agreement, despite it displays a slight skewness towards the lower altitudes. The deviation to the mean is normalized to the standard deviation (30 m) of the distribution. The measurements have been taken during the ELAC campaign (see section 2). The rather symetric distribution indicates a well established decoupling of the stratocumulus deck (base above 2 km) from the boundary layer (0.7 km). On the contrary, a dense cumulus deck over land at the top of a convective boundary layer displays a large bias toward the higher altitude while the planetary boundary layer height in cloud free areas displays a large bias towards the lower altitude indicating organized secondary circulation and a strong coupling.
During ASTEX, transitions in stratocumulus deck from rolls (left) to closed cells (right) were observed as reported on figure 5. The total distance is 85 km. The top altitude varies from 1.25 km to 1.0 km in less than 30 km. In different occasions the cloud top altitude of homogeneous stratocumulus decks varies continuously from 1.4 km to 2 km in a hundred of kilometers.

6. SYNERGISM WITH PASSIVE REMOTE SENSORS

The synergism between lidar and passive remote sensors like infrared radiometers and imager is a key for the definition of future space based payload. Their complementarity is essensial to derive the optical parameters [Flamant et al., 1989] and also to put the lidar measurements on a broader perspective.
The comparison of cloud top height by an airborne lidar (LEANDRE-1) and a narrow field of view IR radiometer (PRT-5) looking at nadir show a good or poor agreement depending on the cloud apparent optical depth (including optical porosity). The top altitudes are in a fair agreement when it is larger than 2 to 3 at 0.53 μm which coresponds to optical depths larger than 1 to 1.5 in the infrared at 10 μm. The measurements were recorded during the ELAC campaign (see section 2).
During EUCREX several flights were conducted on cirrus clouds with LEANDRE-1 and an airborne version of POLDER to study the synergism between the two instruments. POLDER will be launched on ADEOS in 1996. The two instruments were onboard different aircrafts, POLDER looking down and overflying cirrus clouds whereas the lidar was pointing verticaly. The lidar depolarization ratio (Δ) and POLDER informations were used simultaneously to determine the most probable crytal habits for the lidar could provide with two answers for $\Delta \geq 0.24$, either plates or columns. It has been shown that POLDER allows to raise the ambiguity.
During ASTEX the transition between rolls and closed cells were observed by LEANDRE-1 as displayed on figure 5. A SPOT image taken at the same time shows clearly the transition zone and the respective size of closed cells and rolls along the flight track.

7. FUTURE WORKS

Future works to assess the benefit of a backscatter lidar in space will go along the same line as presented above, they will adress the mesoscale variabilities for cloud and aerosols properties. In particular they will adress the correlation between interesting meteorological conditions and optical properties of the atmosphere to be used in meteorological models and the monitoring of the environment. The sampling strategy for a space based backscatter lidar will be conducted in more details in synergy with other remote sensors on board the same platform. Also the lidar signal inversion technique will be investigate to take into account multiple scattering effects and to test new inversion techniques.

Acknowledgment

The authors acknowledge fruitful discussions with their colleagues S. Elouragini, R. Valentin, V. Trouillet, M. Doutriaux, H. Le Treut and G. Sèze. They acknowledge fruitful discussions with G. Brogniez and H. Shepfer.
The work was supported by INSU/CNRS, CNES, the European Space Agency and European Community.

REFERENCES

Ansmann A., J. Bosenberg, G. Brogniez, S. Elouragini, P. H. Flamant, K. Klapeck, H. Linné, L. Menenger, W. Michaelis, M. Riebesell, C. Snneff, P-Y. Thro, U. Wandinger, C. Weitkamp, **1993**, Lidar network observations of cirrus morphological and scattering properties during the International Cirrus Experiment'89 : the 18 October 1989 case study and statistical analysis, 1993, *J. Appl. Meteor.*, vol. 32, pp. 1608-1622.

Brogniez G., H. Chepfer, Y. Fouquart, J-F. Gayet, P. H. Flamant, R. Valentin, J. Pelon, V. Trouillet, C. Flamant, F. Albers, Radiative properties of cirrus clouds observed during the European Radiation Experiment (EUCREX'94) in Brittany by active and passive remote sensing observations, **1995**, EUROPTO : Satellite remote sensing II, Paris, France, 25-28 September.

Elouragini S., P. H. Flamant, J. Pelon, CIRREX'93 : one year lidar monitoring of optical and geometrical properties of mid-latitude cirrus clouds, **1996**, submitted to *Annales Geophysicae*.

Flamant P. H., G. Brogniez, M. Desbois, Y. Fouquart, J-F. Flobert, J-C. Vanhoutte, **1989**, High altitude cloud observation by ground-based lidar, IR-radiometer and Meteosat imagery, *Ann. Geophysicae*, vol. 7, pp. 1-10.

Flamant P. H., J. Pelon, Cloud properties and statistics derived by lidar and infra-red radiometry for ATLID, Workshop on the "European Lidar Campaign 1990", **1992**, ESTEC, Nooordwijk, The Netherlands, 20 October, ESA publication, esa wpp-49

Flamant P. H., R. Valentin, P. Delville, X. Favreau, J. Pelon, A. Dubreil, V. Trouillet, **1995**, French contribution to E-LITE'94 : ground-based lidar measurements in Palaiseau and Lille, E-LITE Workshop, Florence, Italy, 9-10 November.

Pelon J., P. H. Flamant, M. Meissonnier, **1990**, Conception and operation of the French airborne backscatter lidar LEANDRE, proc. 16th ILRC conference, Zuev ed., Tomsk.

Pelon J, V. Trouillet, C. Flamant, P. H. Flamant, R. Valentin, **1995/1**, French contribution to E-LITE'94 : comparative measurements with airborne backscatter lidar LEANDRE-1, E-LITE Workshop, Florence, Italy, 9-10 November.

Pelon J., M. Desbois, P. H. Flamant, H. Le Treut, G. Sèze, **1995/2**, A study of the potential contribution of a backscatter lidar to climatological studies, ESA Contract AO/1-2668/92/NL/CN, final report.

Platt C. M., S. A. Young, A. Carswell, S. Pal, M. P. McCormick, D. M. Winker, F. DelGuasta, L. Stefanutti, W. Eberhard, M. Hardesty, P. H. Flamant, R. Valentin, B. Forgan, G. Gimmestead, H. Jäger, S. S. Khmelevtov, I. Kolev, B. Karielolev, D. Lu, K. Sassen, V. Shamanaev, O. Uchino, Y. Mizuno, U. Wandinger, C. Weitkamp, A. Ansmann, C. Wooldridge, **1994**, The experi-mental Cloud Lidar Pilot Study (ECLIPS) for cloud-radiation research, *Bull. Amer. Meteorol. Soc.*, vol. 75, pp. 1635-1654.

Valentin R., S. Elouragini, P. H. Flamant, L. Menenger, J. Pelon, **1993**, ECLIPS phase 2 at LMD, Optical Remote Sensing of Atmosphere, Salt lake City, Utah, USA, March.

Weill A., F. Baudin, H. Dupuis, L. Eymard, J. P. Frangi, E. Gérard, P. Durand, B. Benech, J. Dessens, A. Druilhet, A. Réchou, P. H. Flamant, S. Elouragini, R. Valentin, G. Sèze, J. Pelon, C. Flamant, J. L. Bringuier, S. Planton, J. Rolland, A. Brisson, J. Leborgne, A. Marsouin, T. Moreau, K. KatsarosS, R. Monis, P. Queffeulou, T. Tournadre, P.K.Taylor, E. Kent, R. Pascal, P. Schibler, F. Parol, J. Descloitres, J. Y. Ballois, M. André, M. Charpentier, **1996**, SOFIA 1992 experiment during ASTEX, Accepted for publication at *The Global Atmosphere and Ocean System.*

Table 1. Parameters of statistical distributions for cirrus altitude, geometrical thickness, and optical parameters at 0.53 μm.

Cirrus parameter	Daily average Minimum	Daily average Maximum	Yearly averaging	Standard deviation	Normalized standard deviation
base (km)	5.0	11.0	8.0	1.7	0.21
top (km)	8.0	13.0	10.8	1.3	0.12
geometrical thickness (km)	0.50	6.0	2.8	1.5	0.54
extinction coefficient (m^{-1})	0.010	0.42	0.079	0.046	0.58
backscatter coefficient (m^{-1})	0.001	0.025	0.0047	0.0027	0.57
optical depth	0.10	1.2	0.25	0.15	0.60

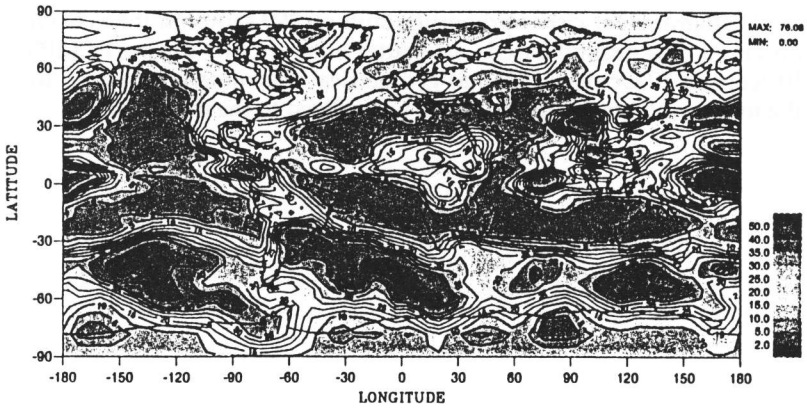

(a) Model

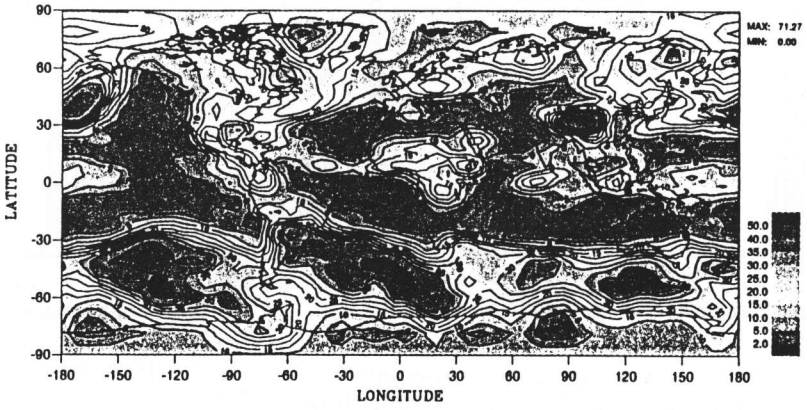

(c) SNR limited lidar

Figure 1 : Comparison of large scale cloudiness for cirrus at 9.8 km, provided by the LMD GCM, and the cloudiness which is retrieved by an orbiting backscatter lidar with ± 23° cross track scanning capability. a) the « true » cloudiness built by the GCM, b) cloudiness retrieved by the lidar according to a SNR=4 detection threshold.

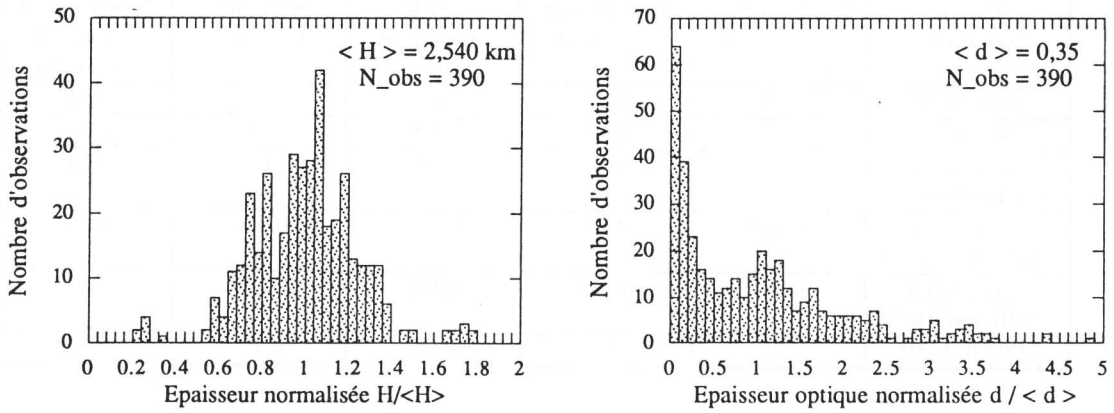

Figure 2 : Histograms for cirrus properties built on 390 samples. It has been observed by a ground based backscatter lidar at LMD during ECLIPS III (case of 10 October 1994). a) geometrical thickness normalized to the mean = 2.5 km, b) optical depth normalized to the mean = 0.35.

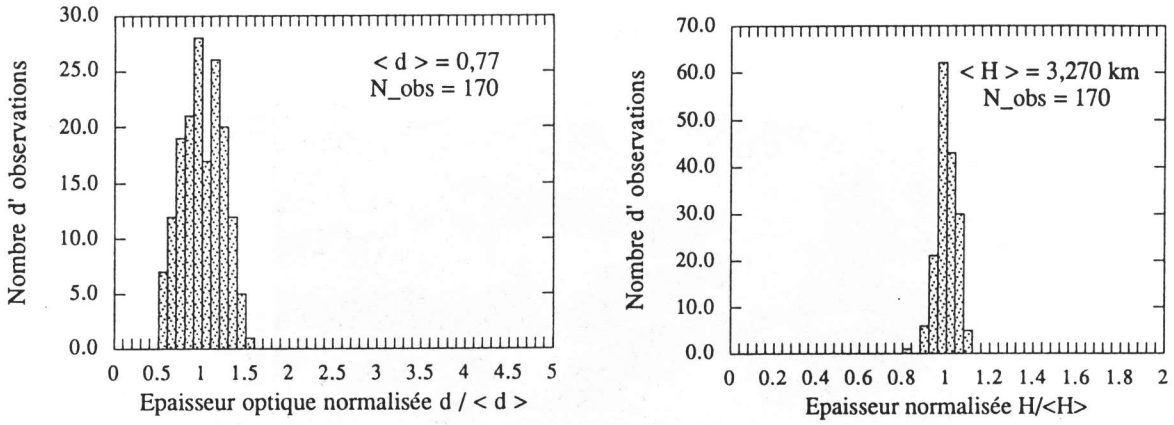

Figure 3 : Histograms for cirrus properties built on 170 samples. It has been observed by a ground based backscatter lidar at LMD during ECLIPS III (case of 11 October 1994). a) geometrical thicknness normalized to the mean = 3.3 km, b) optical depth normalized to the mean = 0.77.

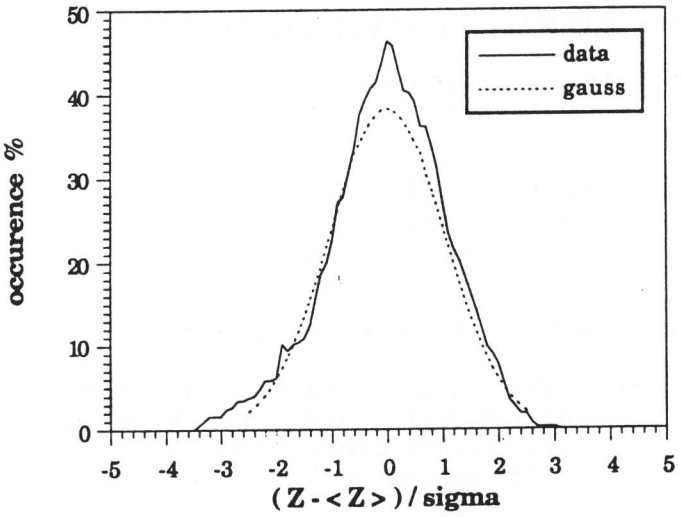

Figure 4 : Histograms of cloud top for a dense stratocumulus layer recorded during ASTEX'92. The statistical distribution is displayed as solid line, the variation to the mean $(z-\langle z\rangle)$ are normalized to the standard deviation of the distribution $\sigma = 30\,\mathrm{m}$. A gaussian distribution (dashed line) with $\sigma = 30\,\mathrm{m}$ is shown for comparison.

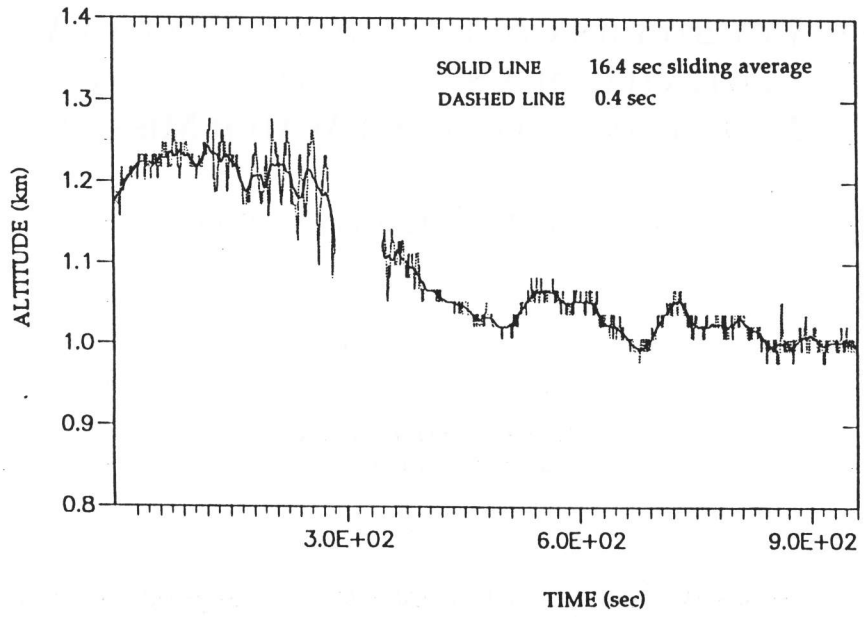

Figure 5 : Transition in stratocumulus layer from rolls (left) to closed cells (right) as observed during ASTEX'92. The total distance is 85 km.

SPACE BASED BACKSCATTER LIDAR

ATLID, ATMOSPHERIC LIDAR
ON-GOING ESA PROJECT

"CLOUD RADIATION MISSION"
NEW ESA PROJECT
INVOLVES ATLID AND OTHER SENSORS

SPACE BASED DIAL-WATER VAPOR LIDAR

BEST, ENERGY BUDGET OF THE TROPICAL SYSTEM
- DEFINITION STUDY FOR MULTI SENSOR PAYLOAD
WIND DOPPLER LIDAR, RAIN RADAR, ...
A REPORT WAS ISSUED BY CNES IN 1989

SIMULTANEOUS DIAL WATER VAPOR AND WIND DOPPLER MEASUREMENTS
- ON-GOING ESA PROJECT

OVERVIEW OF STUDIES CONDUCTED IN FRANCE TO ASSESS THE POTENTIAL OF A SPACE BASED LIDAR FOR RADIATION AND CLIMATE WATCH MISSION

Pierre H. Flamant and Jacques Pelon

Laboratoire de Meteorologie Dynamique du CNRS
Ecole Polytechnique, France

Service d'Aeronomie du CNRS
Universite Paris-6, France

International Workshop on Spaceborne Lidar 1995 - Technology and Applications
Nara, Japan, 24-26 October, 1995

SPACE BASED BACKSCATTER LIDAR

VARIOUS TYPES OF SCIENCE STUDY

- GLOBAL SCALE LIDAR SIMULATOR

  ORBITING LIDAR INSTRUMENT
  LARGE SCALE CLOUDINESS (MANY LAYERS)

- FIELD EXPERIMENTS

  LIDAR DATA AT SMALL-SCALE AND MESO-SCALE

- LIDAR INVERSION METHOD

  RETRIEVAL OF BACKSCATTER / EXTINCTION COEFFICIENTS
  MULTIPLE SCATTERING

FUNDING AGENCIES

- CNES / FRENCH SPACE AGENCY
- ESA / EUROPEAN SPACE AGENCY
- CNRS / NATIONAL CENTER FOR SCIENTIFIC RESEARCH
- EC / EUROPEAN COMMUNITY

SPACE BASED BACKSCATTER LIDAR

OBJECTIVES

- MONITORING OF THE ENVIRONMENT
- CLIMATE CHANGE, VARIABILITY AND DYNAMICS
- RADIATIVE TRANSFERT IN THE ATMOSPHERE
- CLOUD-RADIATION INTERACTION
- TRANSPORT

PARAMETERS OF INTEREST

- LARGE SCALE CLOUDINESS
  STRATIFORM VS. CONVECTIVE CLOUDS
  HOMOGENEOUS VS. BROKEN CLOUD FIELDS

- CLOUD RADIATIVE PARAMETERS
  3D-STRUCTURE
  OPTICAL PROPERTIES
  ICE/WATER DISCRIMINATION
  MICROPHYSICS (LWC, Re)

- PLANETARY BOUNDARY LAYER HEIGHT

END-TO-END SIMULATION

PERFORMANCE ON LIDAR LINE-OF-SIGHT

SHOT AVERAGING

VERTICAL AND HORIZONTAL RESOLUTION

SAMPLING CAPABILITY

LIDAR INSTRUMENT

ORBITING PLATFORM (HEIGHT, INCLINAISON)

SNR FOR RELIABLE DETECTION (ENERGY x COLLECTING AREA)

CROSS-TRACK SCANNING (COVERAGE)

LARGE SCALE CLOUDINESS

ISCCP C1-DATA= REALISTIC CLOUDINESS

LMD GCM OUTPUTS = CONSISTENT METEOROLOGICAL FIELDS
(CLOUDS, RADIATIVE FLUXES, WATER VAPOR, WIND),

SAMPLING STRATEGY

CLOUDS ⇨ TARGETS & OBSTRUCTION

LIDAR DEALS WITH SMALL SCALE CLOUDINESS
NO SUCH A DATA BASE AVAILABLE

SATELLITE OBSERVATIONS

⇨ LARGE SCALE (TIME / SPACE) CLOUDINESS
50 to 60 % CUMULATED CLOUDINESS
GLOBAL Ci COVER

ANALYSIS

ISCCP C1 DATA MONTHLY AVERAGE JULY 1986

7 LAYERS , 2.5° x 2.5° PIXEL

CUMULATED CLOUDINESS BROKEN DOWN IN FRACTIONAL LAYER CLOUDINESS (CLASSIFICATION ALGORITHM)

ORBITING LIDAR ⇨ H, ξ, θ, PRF, T_S or T_D
LIDAR LOS IN LOWER ATMOS. ASIGNED TO A SINGLE PIXEL

UNIFORM RANDOM SIMULATOR ⇨ x in [0 , 1] interval
$x >$ **cumulated cloudiness ⇨ clear ⇨ free shot**
$x \leq$ **cumulated cloudiness ⇨ cloud ⇨ blocked shot**

Decorrelated cloudiness from layer to layer

OUTPUT

LIDAR SHOT DENSITY IN 100 x 100 km^2 AREA

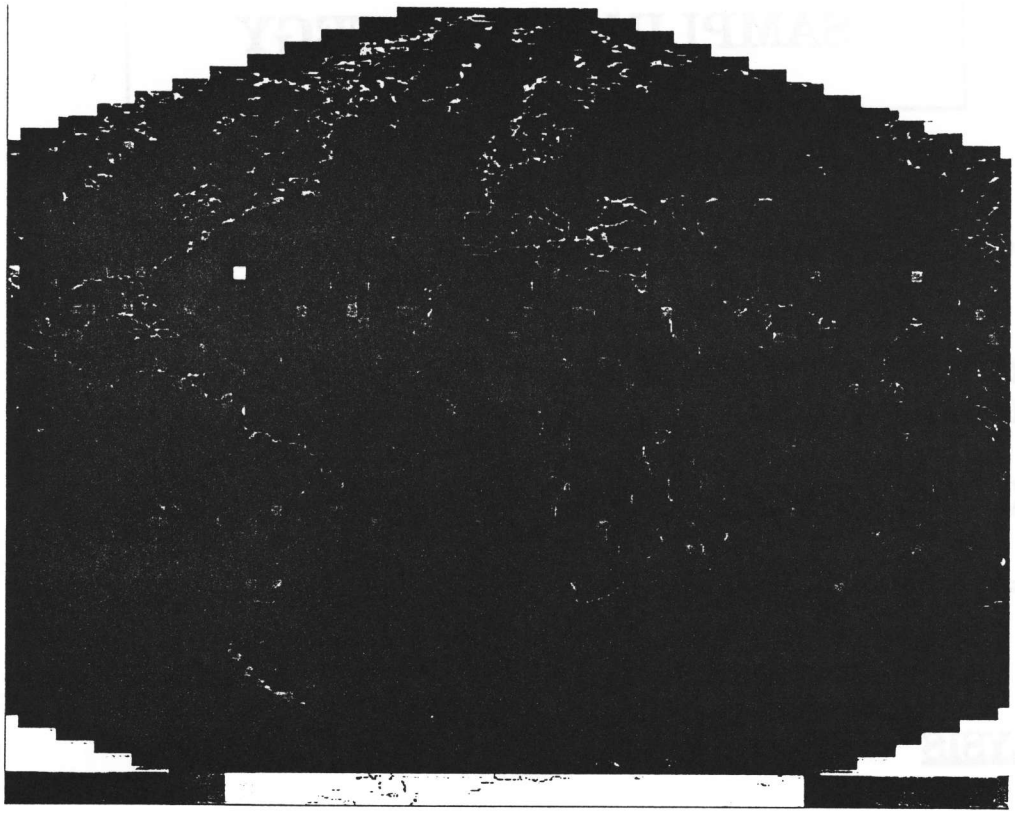

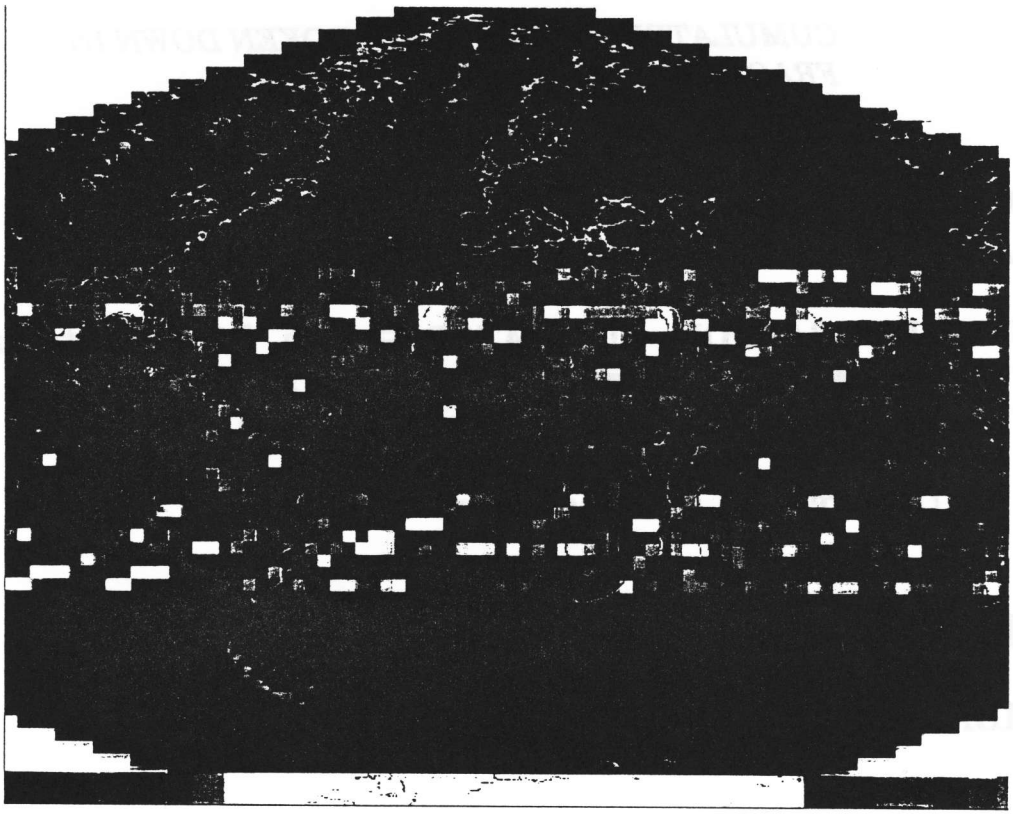

The LMD GCM model

The grid

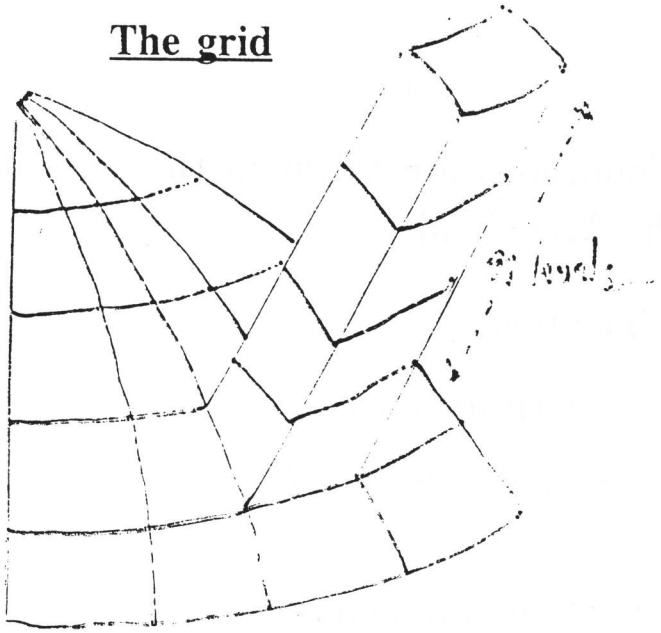

Horizontal

equal area — 64 points in longitude.
50 points in sine of latitude.

Vertical

11 σ levels — 4 PBL
4 Troposphere
3 Stratosphere

Time-step

Dynamic: 6 minutes
Physic : 30 minutes
Radiation: no diurnal cycle

This model was used to analyse the sensitivityof radiation fluxes at the TOA and at the surface for different τ of high level clouds.

Conditions are taken in the 3D calculations performed with LMD GCM

- The point
  - latitude 35.4°
  - longitude -81.54°

- Surface parameters
  - P_s=974 hPa, T_s=297.6 K
  - albedo 0.15
  - temperature, water vapor, and liquid water content vertical profils are those coming from the GCM
- other parameters
  * r_e=10 μm
  * solar constant=1370 W/m^2

Sensitivity of radiation fluxes at the surface and at the TOA for different optical thickness (τ) of high clouds.

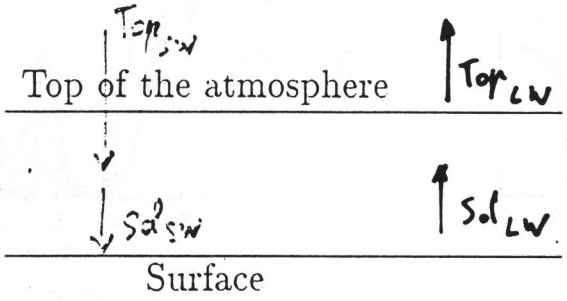

Net radiative flux at the TOA

Distribution	TOP_sw (W/m^2)	TOP_lw (W/m^2)	Net flux (W/m^2)
Clear sky	408	281	127
τ=0.1	405	276	130
τ=0.3	400	262	138
τ=0.5	395	250	145

Net radiative flux at the Surface

Distribution	SOL_sw (W/m^2)	SOL_lw (W/m^2)	Net flux (W/m^2)
Clear sky	310	63	247
τ=0.1	306	62	244
τ=0.3	301	61	240
τ=0.5	296	59	237

WE MUST DETECT CLOUDS WITH $\tau > 0.3$

HIGH LEVEL CLOUDS

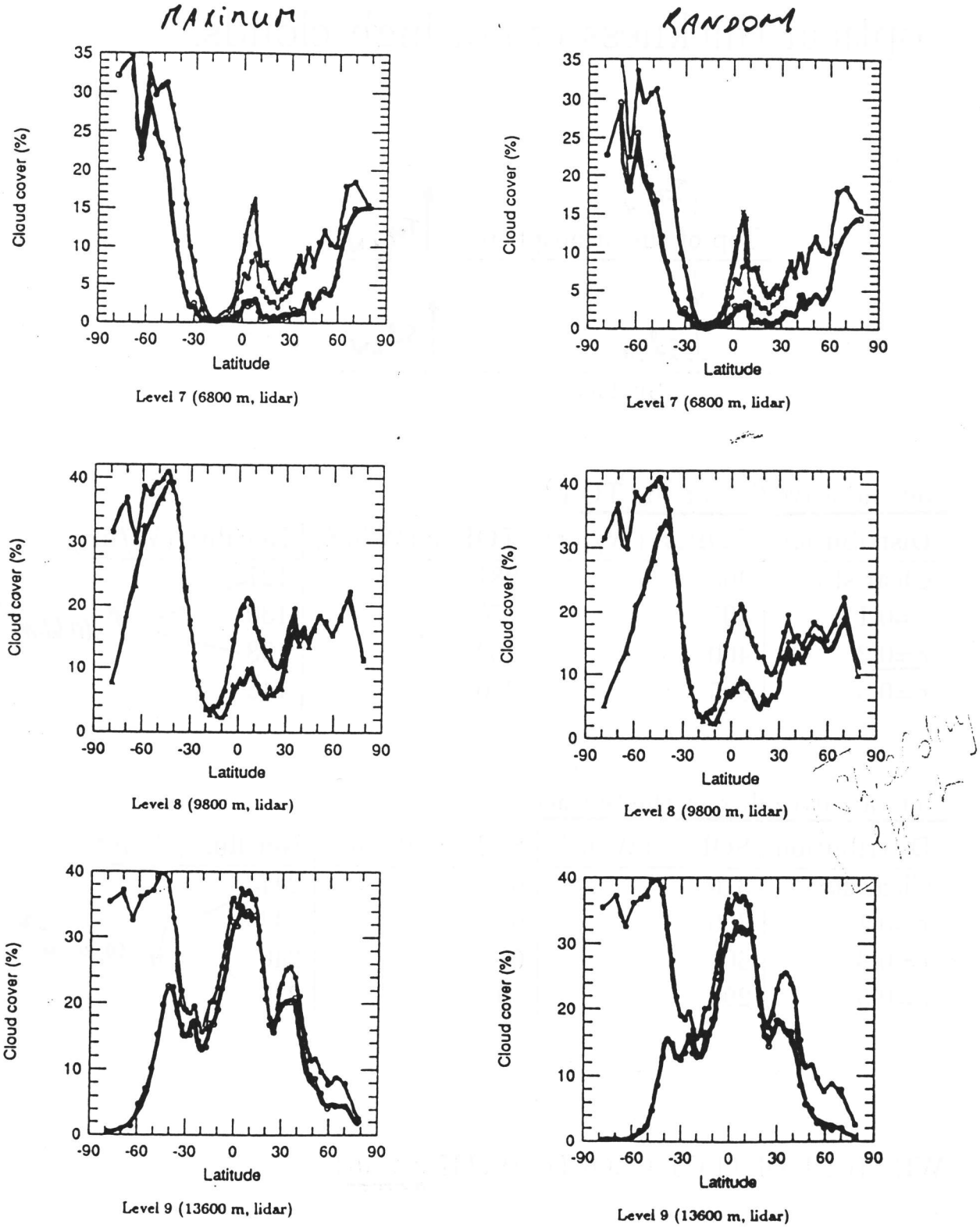

Figure 4.4 : Same as figure 4.2

— SAM
— model
— "perfect" lidar

LEVEL 8 (~ 9400 m) July 1987 - Mexi

CLOUD COVER SIMULATED BY LMD GCM

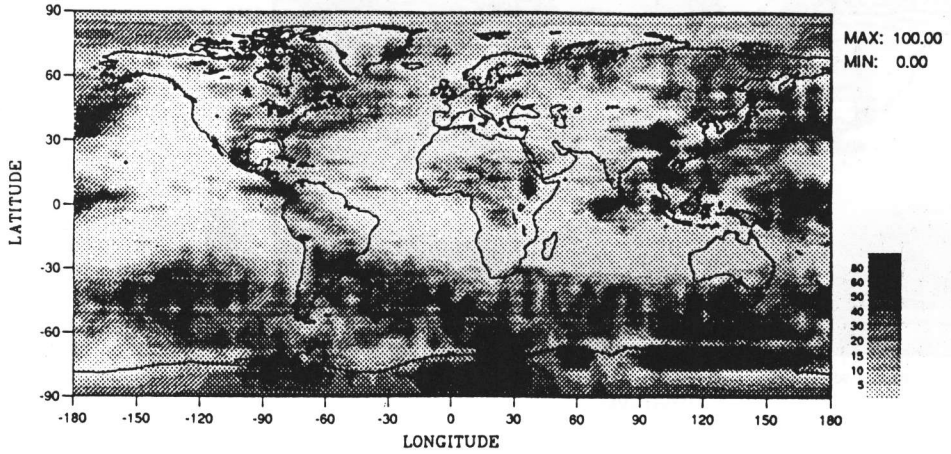

CLOUD COVER AS WOULD BE A "PERFECT" LIDAR

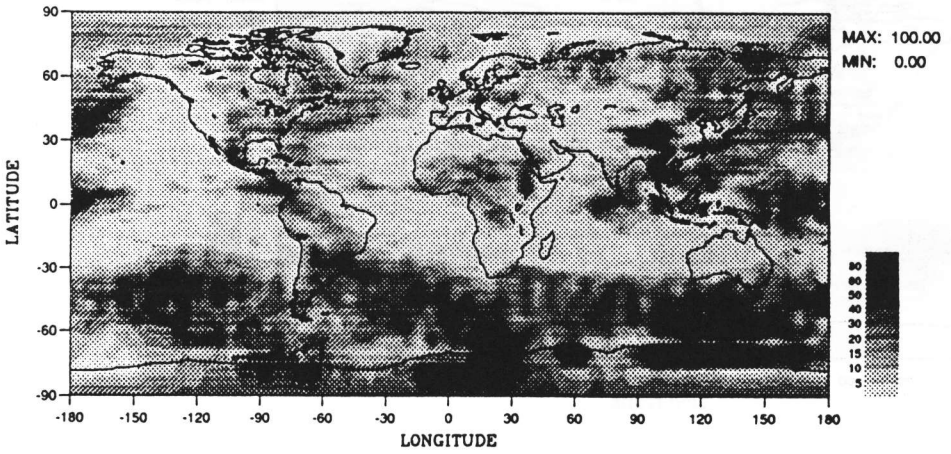

CLOUD COVER AS WOULD SEE A LIDAR (β = 5)

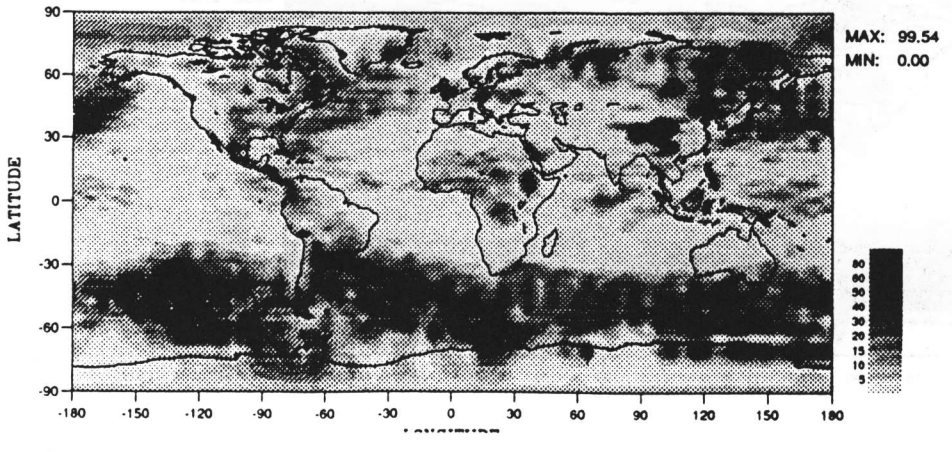

LEVEL 8 (~ 9800 m) July 1987 - Run:

CLOUD COVER SIMULATED BY LMD GCM

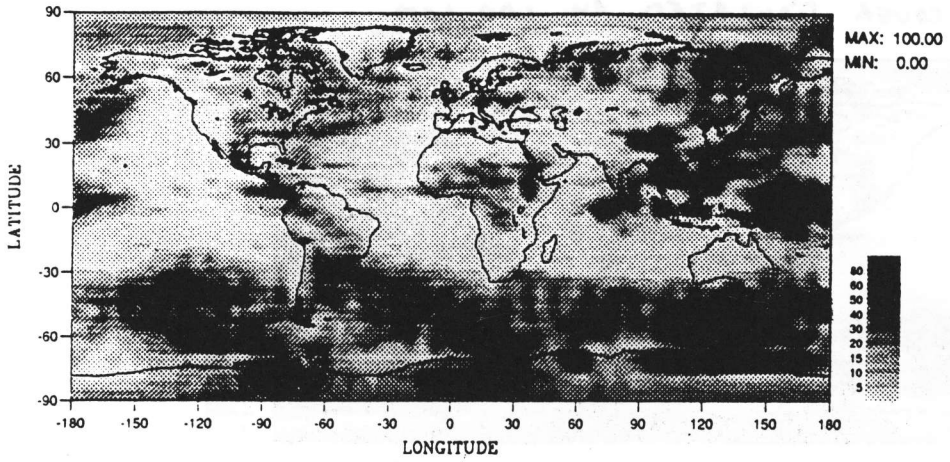

CLOUD COVER AS WOULD REPORT ISCCP WITHOUT VISIBLE CORRECTION

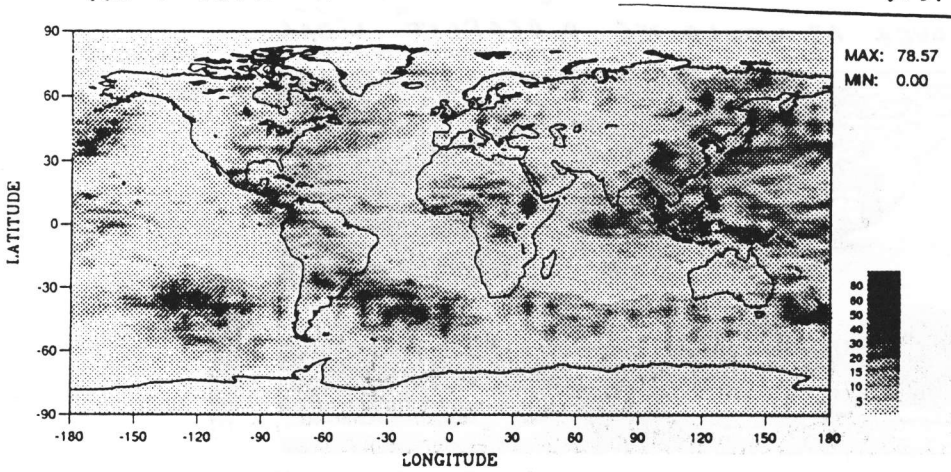

CLOUD COVER AS WOULD REPORT ISCCP

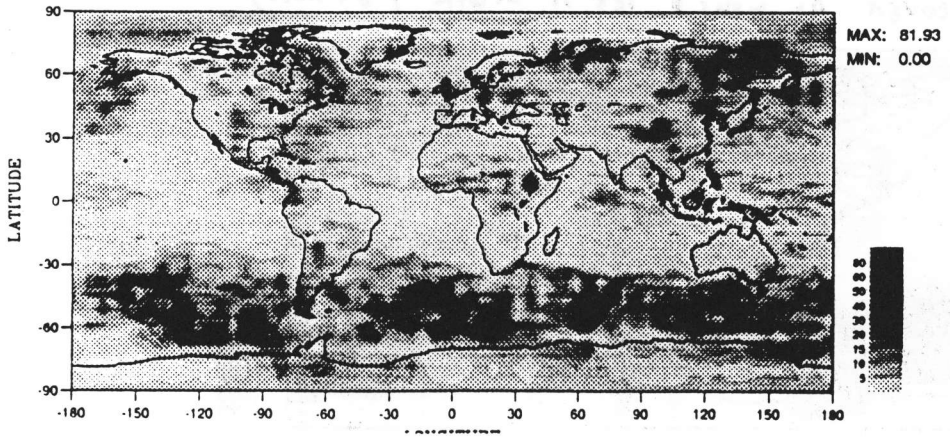

VARIABILITY AT DIFFERENT SCALES

USING LIDAR DATA FROM FIELD CAMPAIGNS

BACKSCATTER LIDAR FIELD CAMPAIGNS

AIRBORNE AND GROUND-BASED LIDARS

1990 OCT.-NOV.	PYREX, PYRENEE EXPERIMENT
	ELAC, EUROPEAN LIDAR AIRBORNE CAMPAIGN
1991 MAY	ECLIPS-2, EXPERIMENTAL CLOUD LIDAR PILOT STUDY
1992 JUNE	ASTEX, AZORES STRATOCUMULUS EXPERIMENT
1993	CIRREX, CIRRUS EXPERIMENT
1994 APRIL	EUCREX, EUROPEAN CLOUD RADIATION EXPERIMENT
1994 SEPT.	E-LITE, EUROPEAN LITE
1994 SEPT.	ECLIPS-3, EXPERIMENTAL CLOUD LIDAR PILOT STUDY

DATA ANALYSIS FOR SPACE APPLICATION

- CLIMATOLOGY OF CLOUD PARAMETERS (MEAN VALUE, STANDARD DEVIATION)
- REPRESENTATIVENESS AT SMALL SCALES (SUB-GRID VARIANCE)
- SYNERGY BETWEEN LIDAR AND PASSIVE SENSORS
- NEW LIDAR INVERSION METHOD

Table 3 : **One year lidar statitics of geometrical and optical properties for mid-latitude cirrus.**

The optical parameters are derived at 0.53 μm. The yearly mean is based on 51 daily recordings, each representing about 100 to 300 lidar files. A file is made of 400 lidar shots taken in one minute. R_B and R_T are the cirrus top height and base height, H is the geometrical thickness, β_A and α_A are the mean backscatter and extinction coefficients averaged on a lidar profile, k is the lidar ratio, δ the optical depth.

Cloud Parameters	Daily minimum	Daily maximum	Yearly mean	Standard deviation	Normalized std
R_B (km)	5.0	11.0	8.0	1.7	21%
R_T (km)	8.0	13.0	10.8	1.3	12%
H (km)	0.5	6.0	2.8	1.5	54%
α_A (km^{-1})	0.010	0.42	0.079	0.046	58%
β_A (km^{-1} sr^{-1})	0.001	0.025	0.0047	0.0027	57%
δ	0.01	1.20	0.25	0.15	60%

Table 4 : **Lidar statistics of lidar ratio for mid-latitude cirrus based on 5 time series during CIRREX'93.**

Cloud Parameters	minimum	maximum	mean	deviation	Normalized Standard deviation
k (sr^{-1})	0.030	0.090	0.060	0.015	25%

→ LIDAR POINTING AT 6° FROM ZENITH

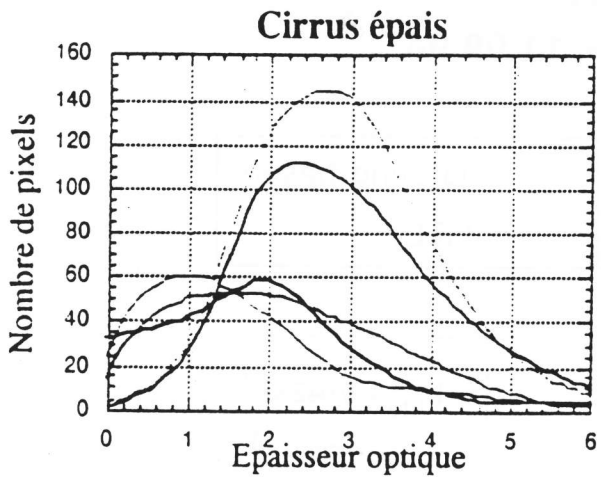
Cirrus épais
Nombre de pixels
Epaisseur optique

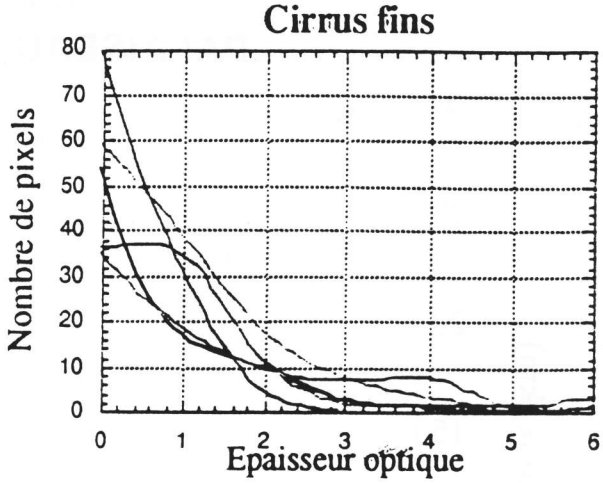
Cirrus fins
Nombre de pixels
Epaisseur optique

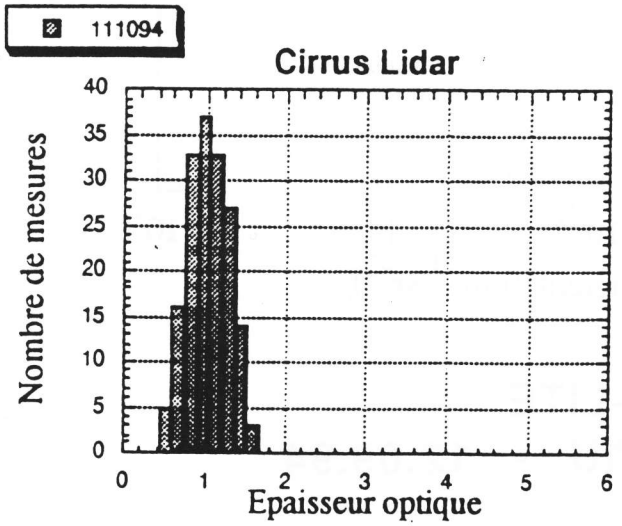
111094
Cirrus Lidar
Nombre de mesures
Epaisseur optique

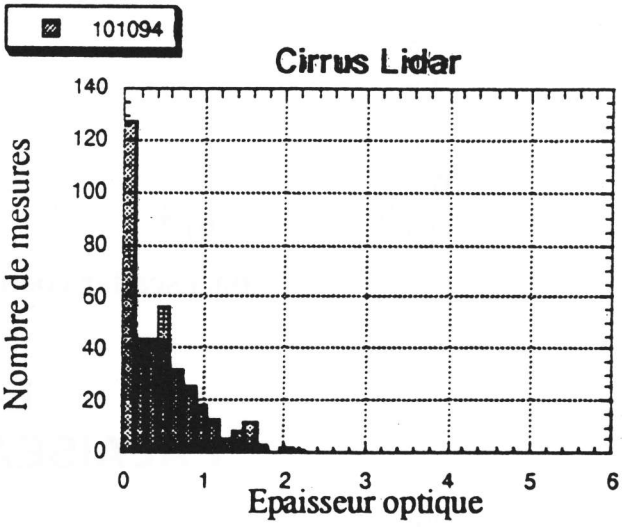
101094
Cirrus Lidar
Nombre de mesures
Epaisseur optique

E-LITE
PALAISEAU - 11.09.94

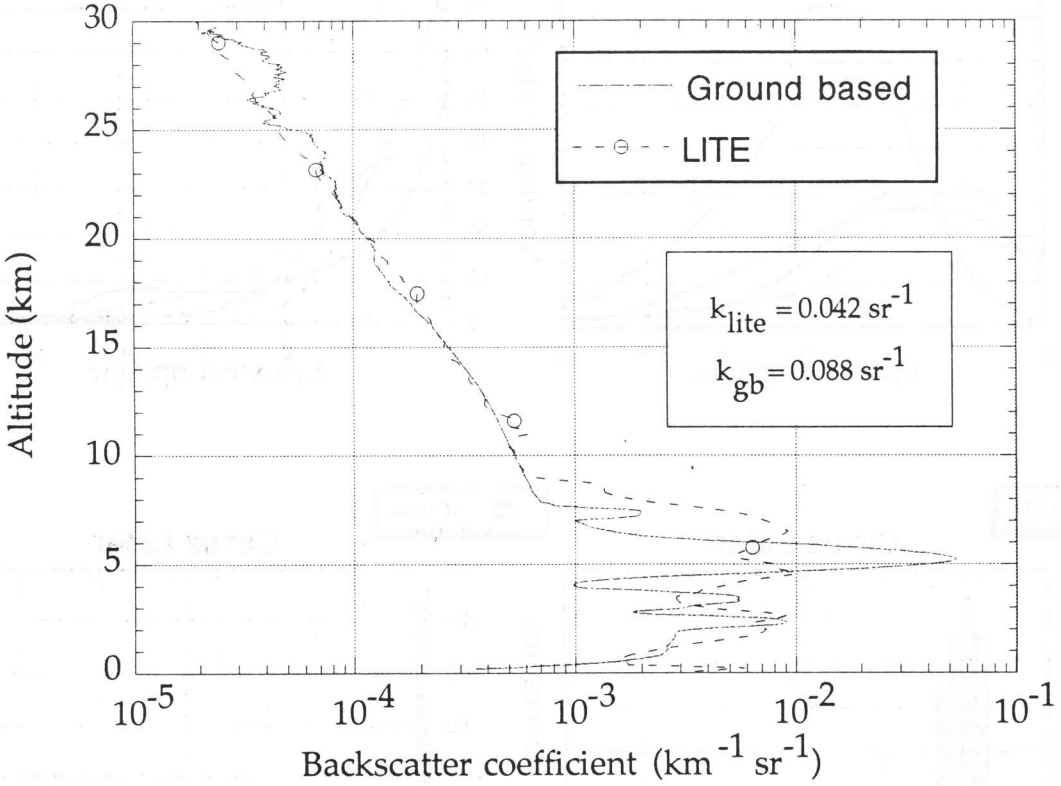

E-LITE
PALAISEAU - 12.09.94

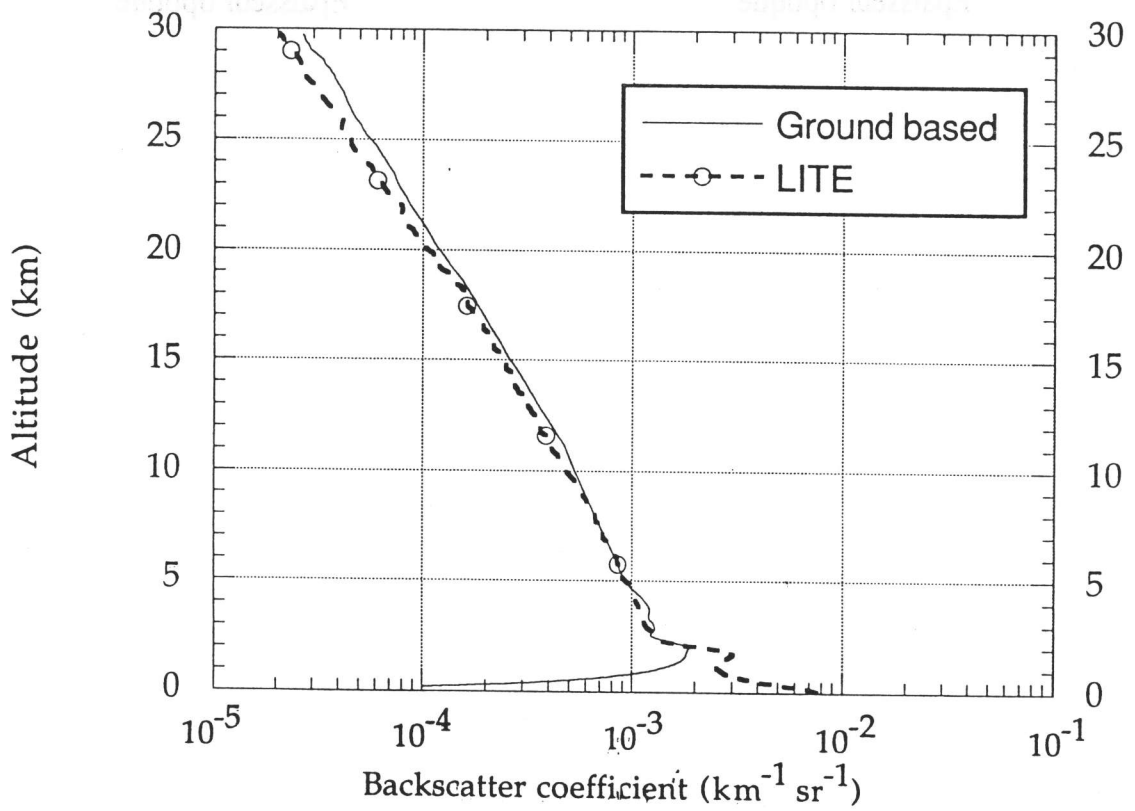

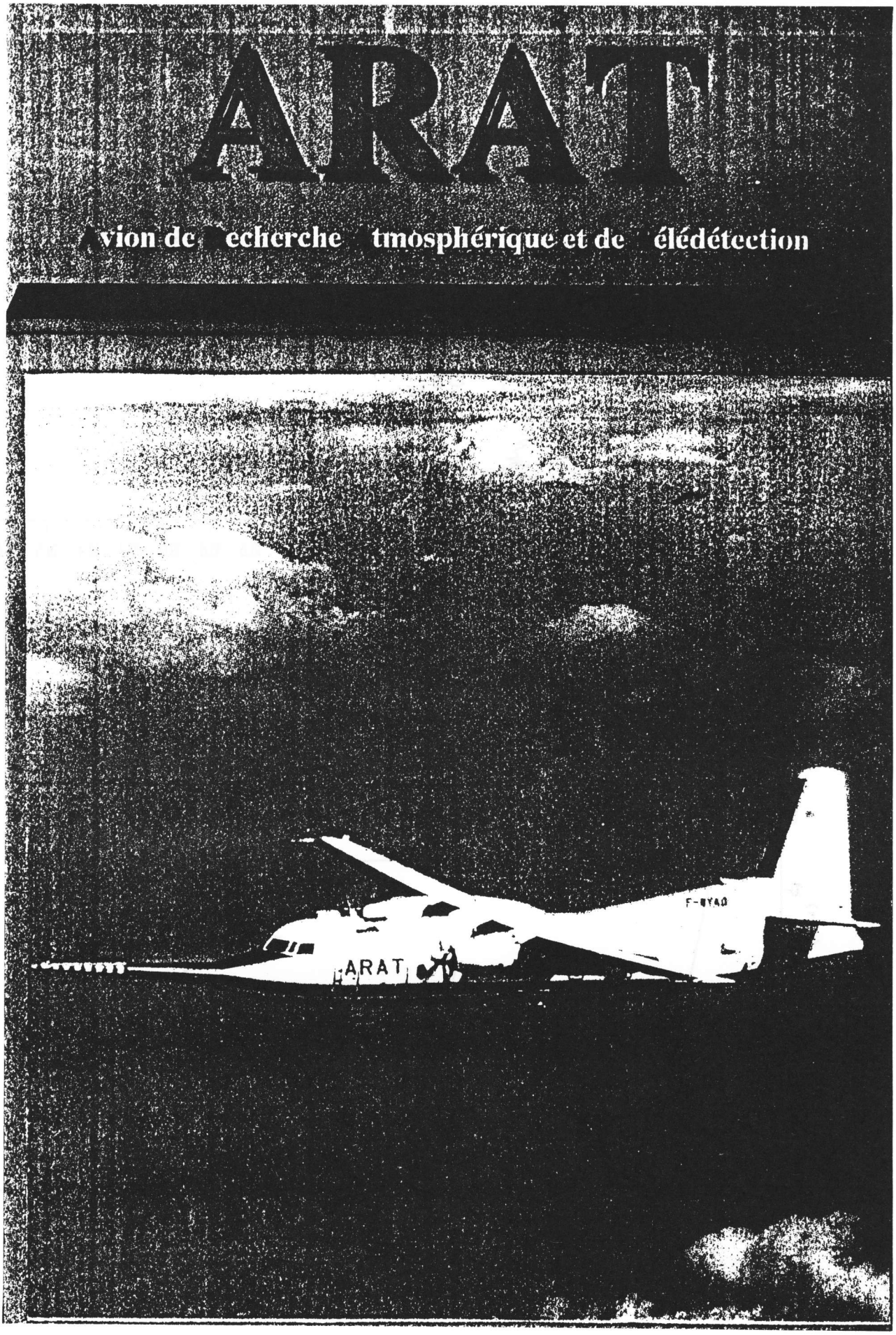
ARAT
vion de echerche tmosphérique et de élédétection
F-GYAQ
ARAT

LITE – SHUTLLE – ORBIT 33

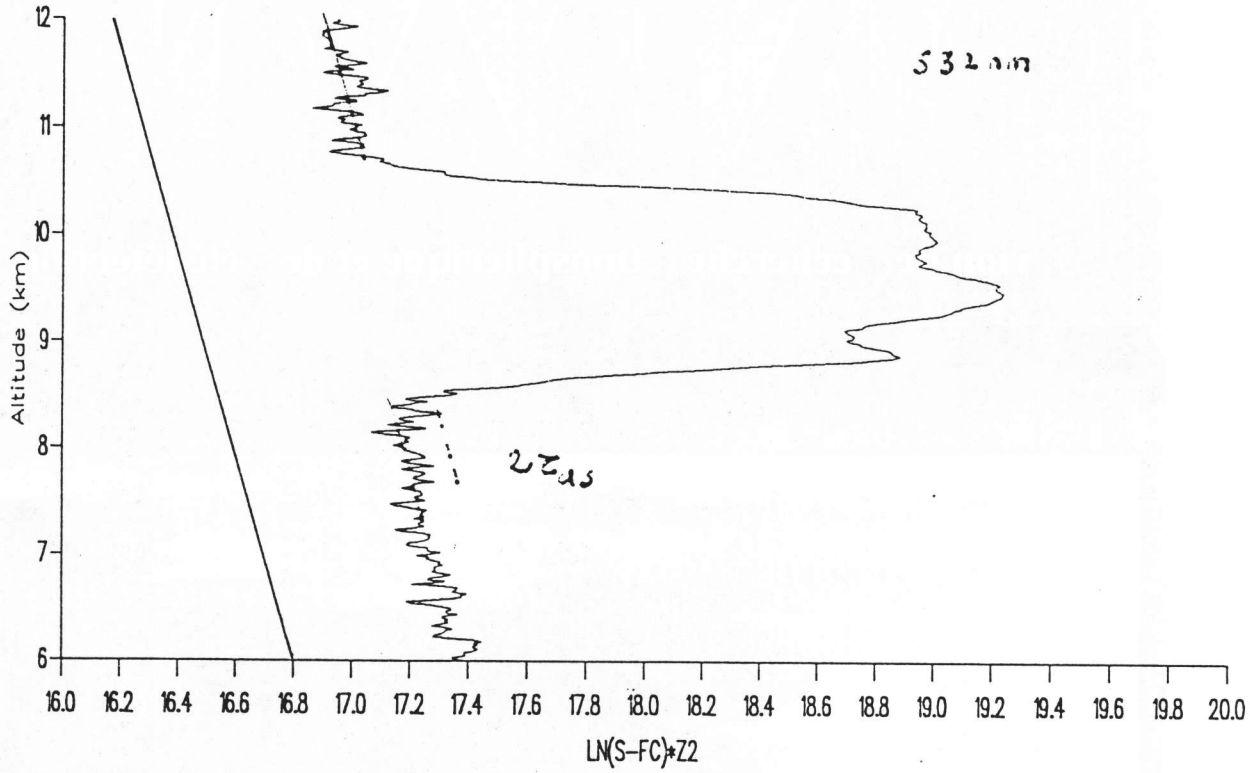

ELITE – ARAT – FLIGHT 21 – ORBIT 33

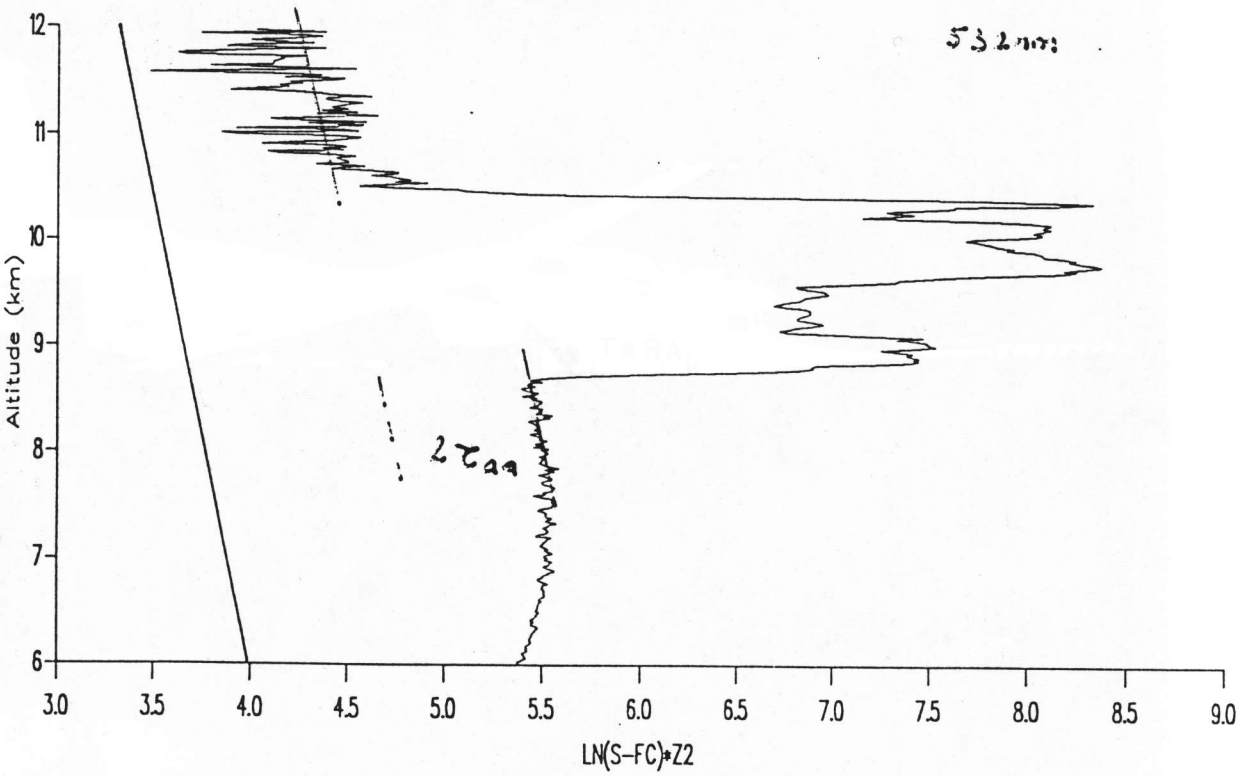

AIRBORNE LIDAR "BACKSCATTER"
FRONT / AZORES
1 TRANSMITTED λ / 1 DETECTION CHANNEL
0.53μm

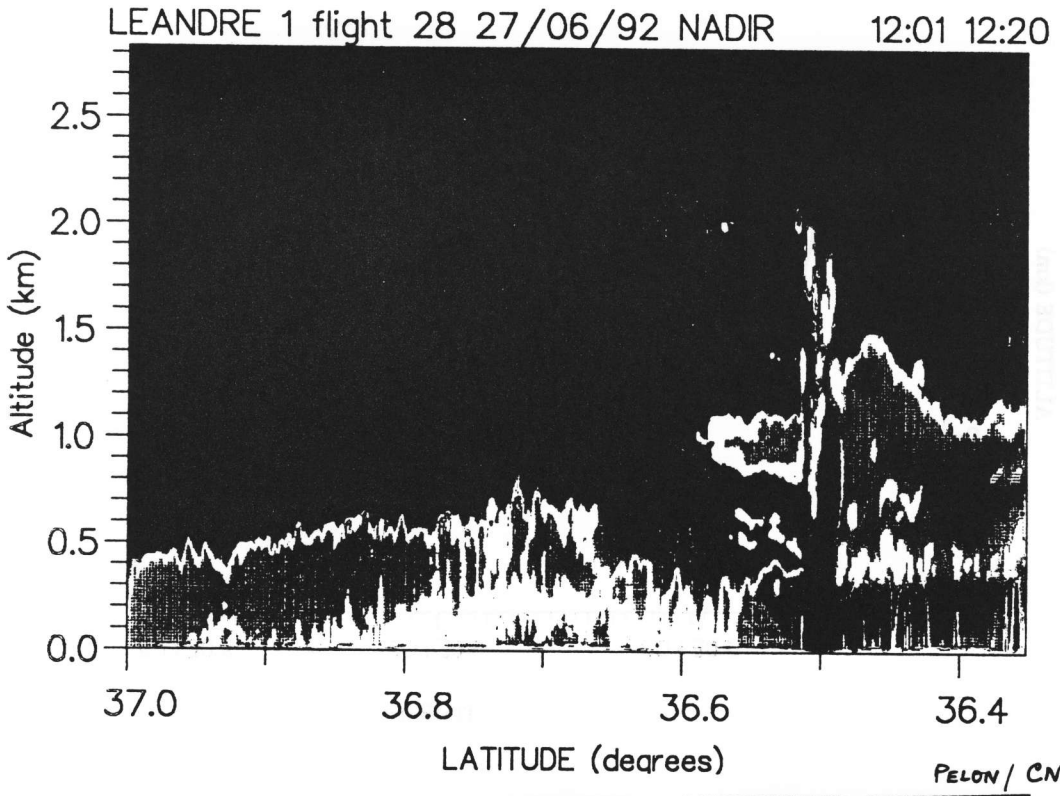

PELON / CNRS

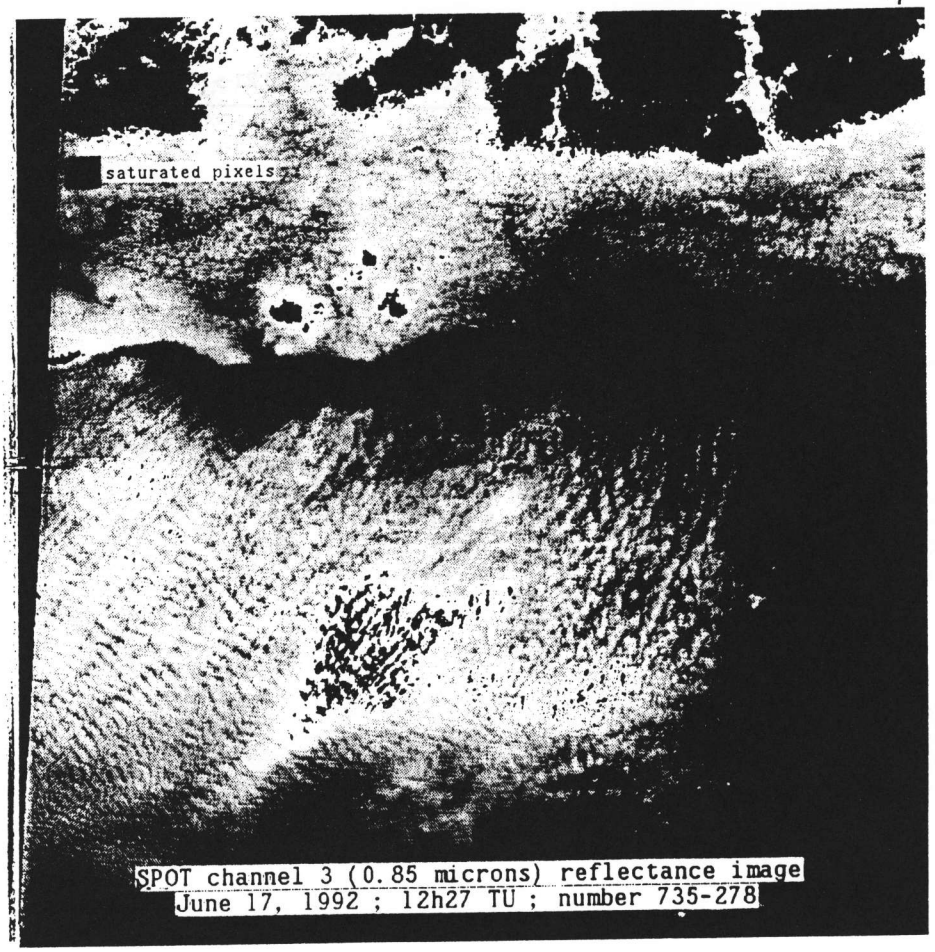

SOFIA-ASTEX

17 JUNE 1992, 11:02 GMT

LEANDRE

BACKSCATTER LIDAR (Nd-YAG, 0.53 μm)

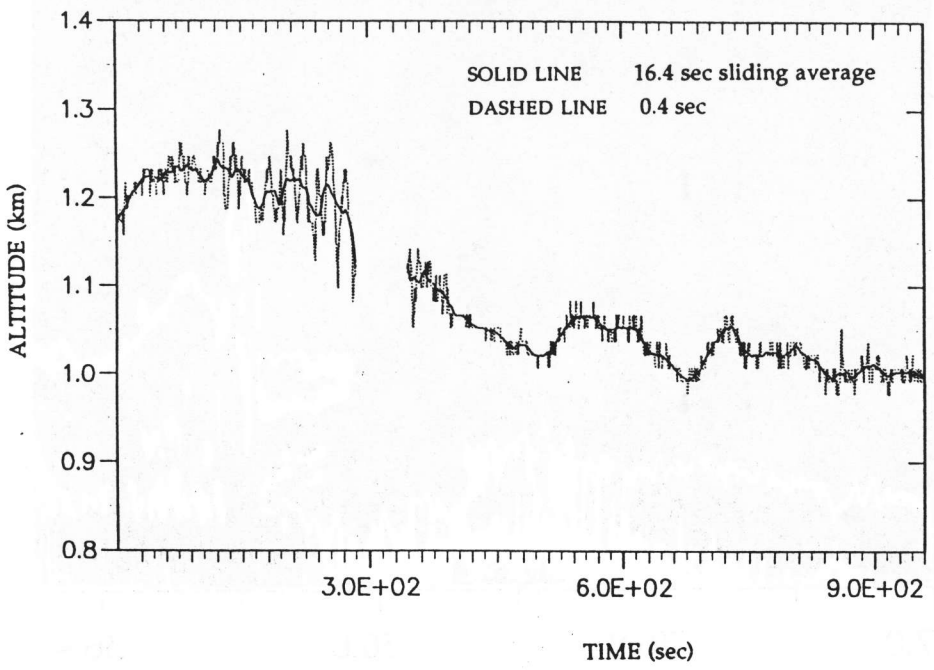

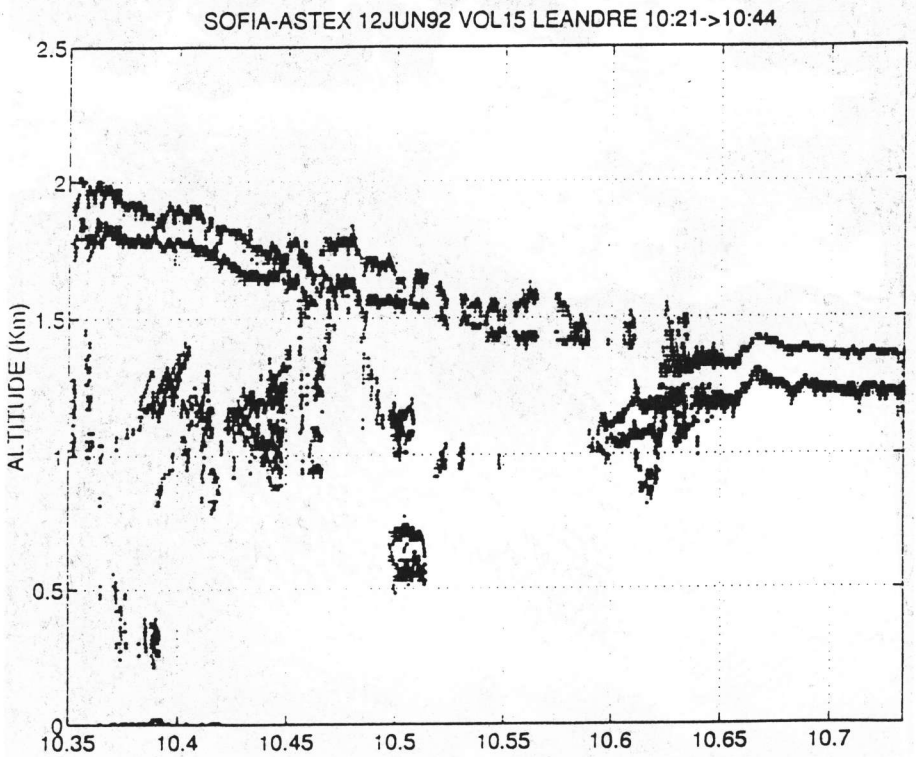

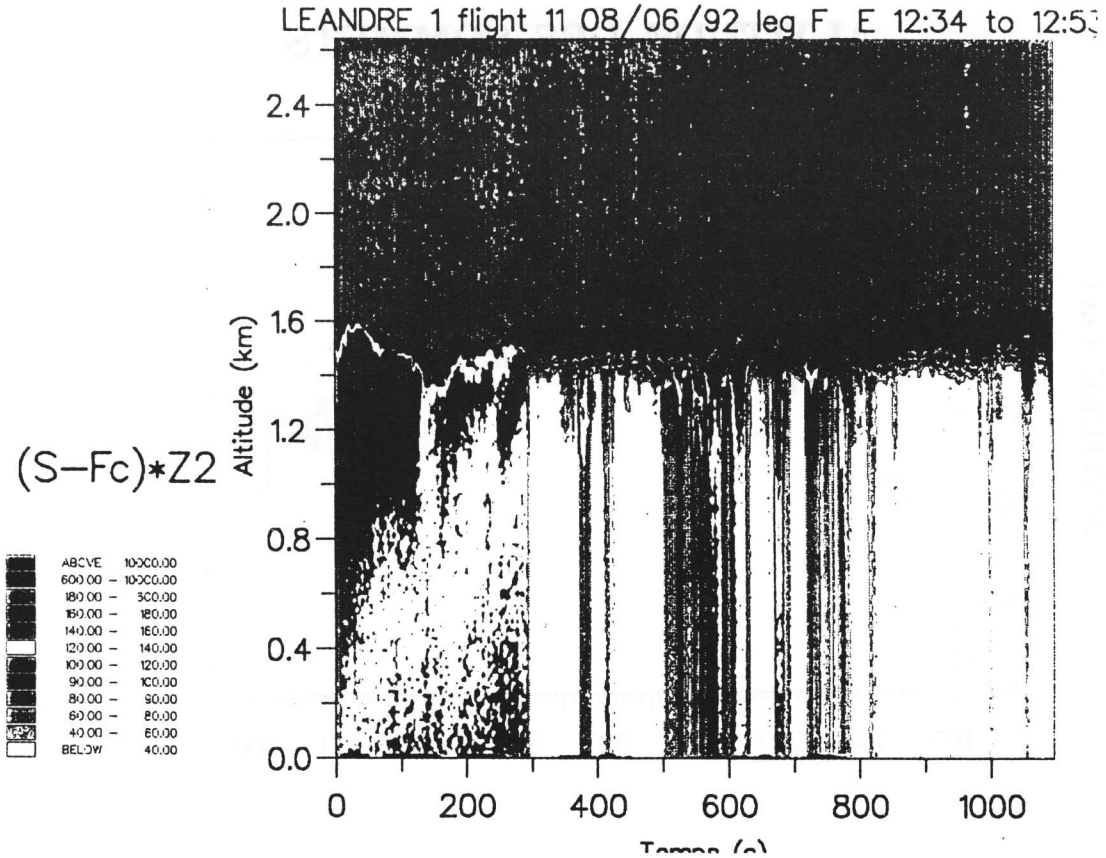
LEANDRE 1 flight 11 08/06/92 leg F E 12:34 to 12:5
(S–Fc)*Z2
ABOVE 1000.00
600.00 – 1000.00
180.00 – 300.00
160.00 – 180.00
140.00 – 160.00
120.00 – 140.00
100.00 – 120.00
90.00 – 100.00
80.00 – 90.00
60.00 – 80.00
40.00 – 60.00
BELOW 40.00
Altitude (km)
0.0
0.4
0.8
1.2
1.6
2.0
2.4
0
200
400
600
800
1000

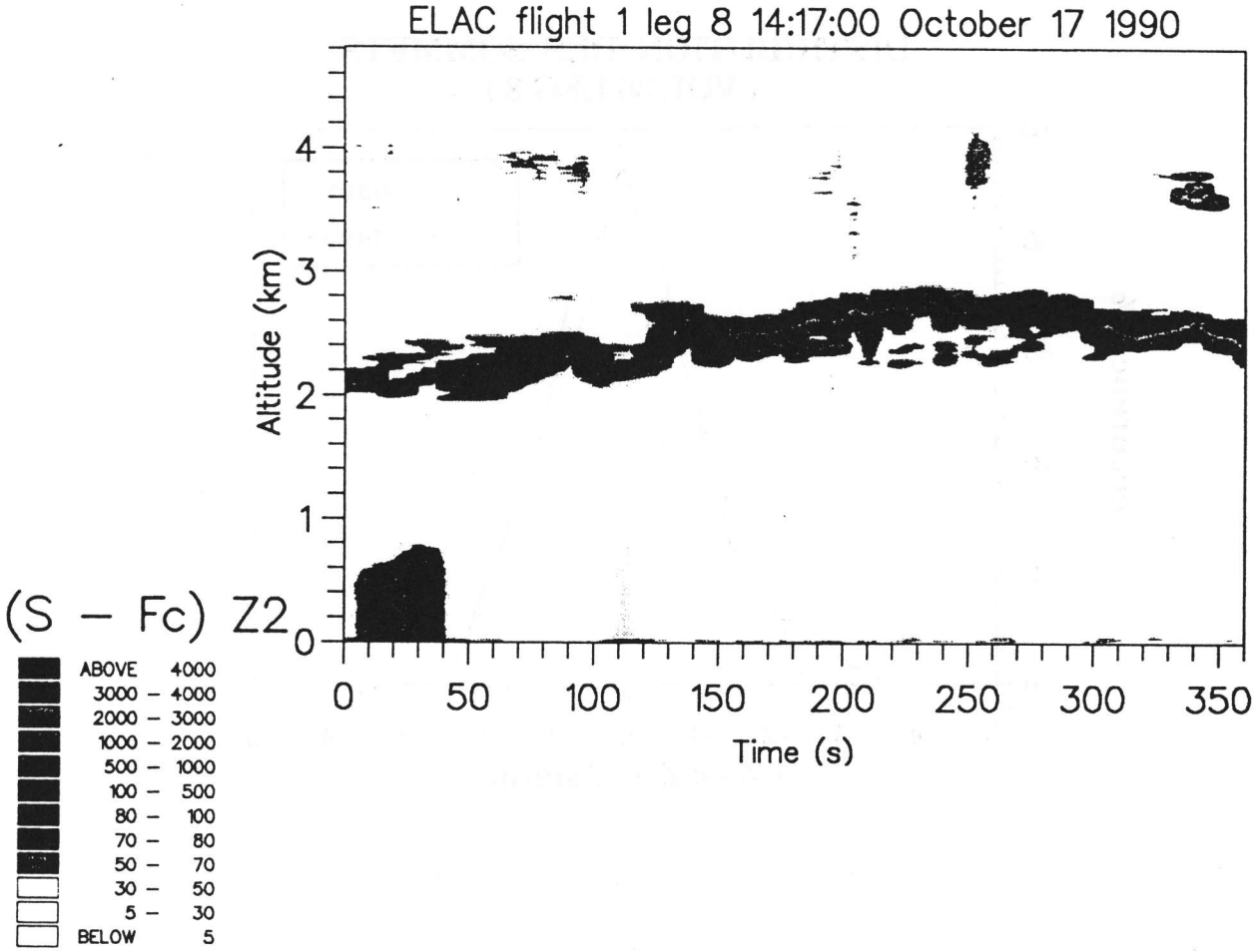
ELAC flight 1 leg 8 14:17:00 October 17 1990
(S – Fc) Z2
ABOVE 4000
3000 – 4000
2000 – 3000
1000 – 2000
500 – 1000
100 – 500
80 – 100
70 – 80
50 – 70
30 – 50
5 – 30
BELOW 5
Altitude (km)
0
1
2
3
4
0
50
100
150
200
250
300
350
Time (s)

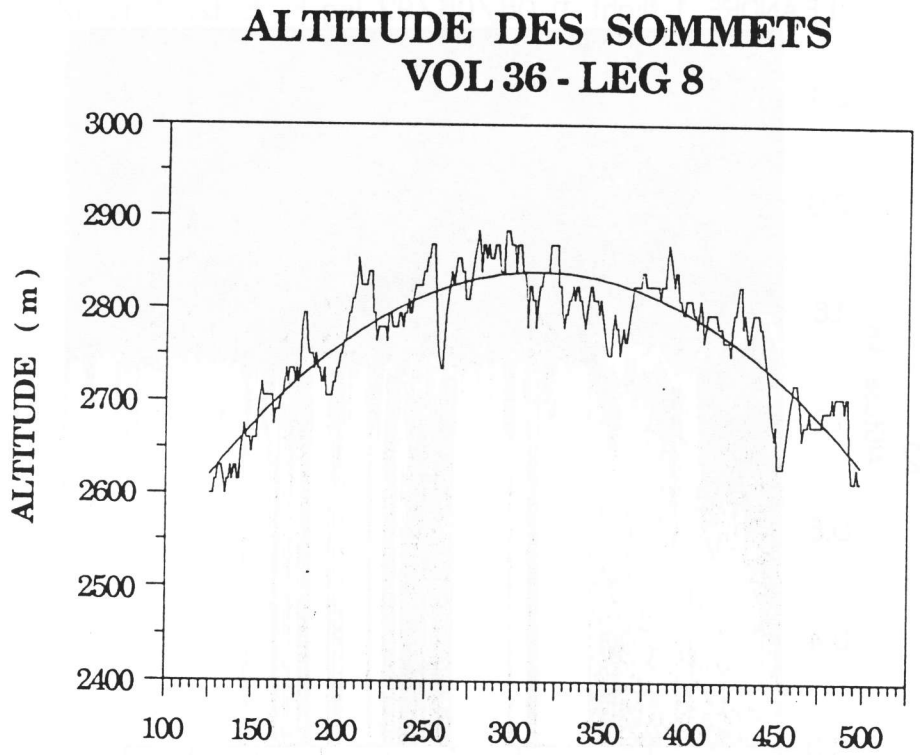
ALTITUDE DES SOMMETS
VOL 36 - LEG 8
ALTITUDE (m)
3000
2900
2800
2700
2600
2500
2400
100
150
200
250
300
350
400
450
500

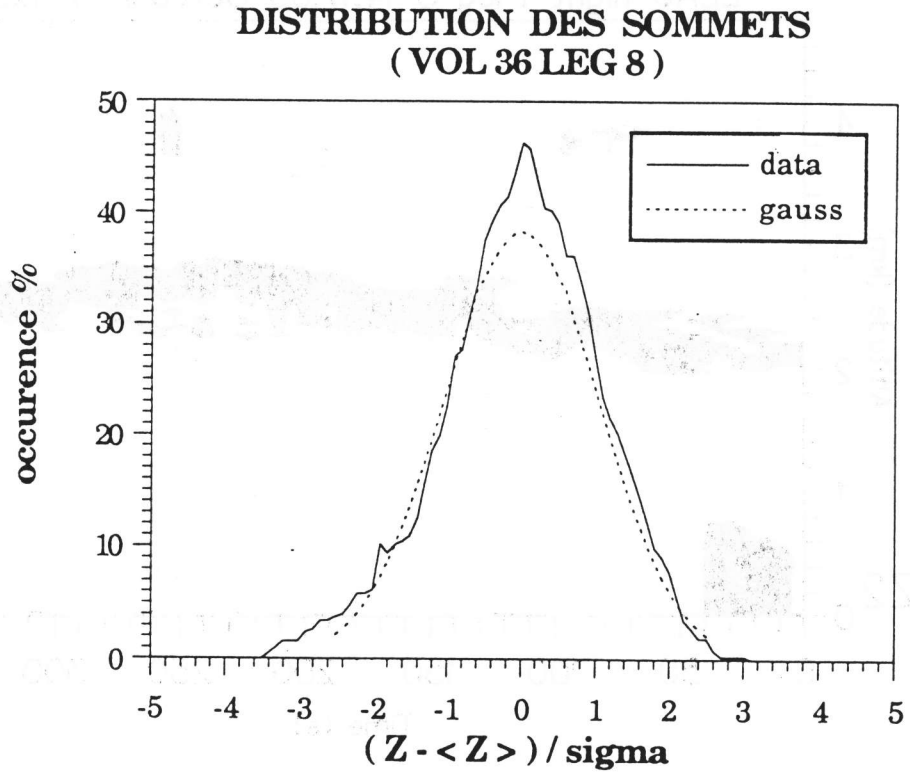
DISTRIBUTION DES SOMMETS
(VOL 36 LEG 8)
occurence %
50
40
30
20
10
0
data
gauss
-5
-4
-3
-2
-1
0
1
2
3
4
5
(Z - < Z >) / sigma

PROBABILITY DENSITY FUNCTION

LEANDRE 1 27/05/91

CLOUD TOP
sampling (1,2 s - 0,1 Km) σ= 30m

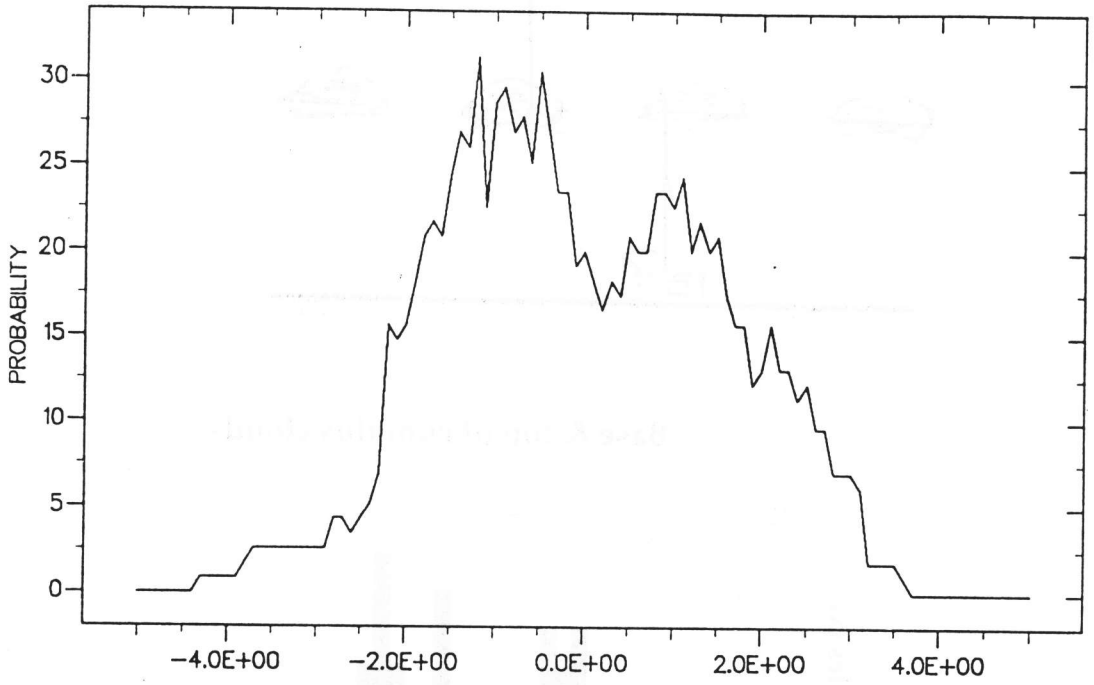

ATMOSPHERIC BOUNDARY LAYER
sampling (1,2 s - 0,1 Km) σ= 30m

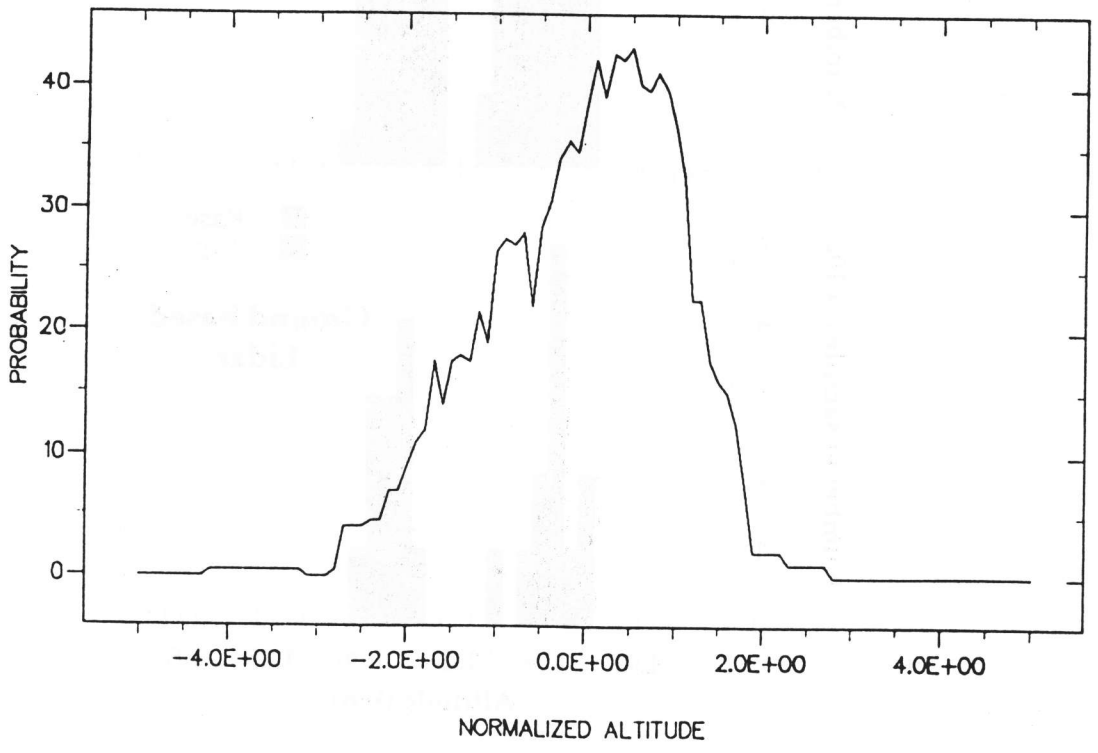

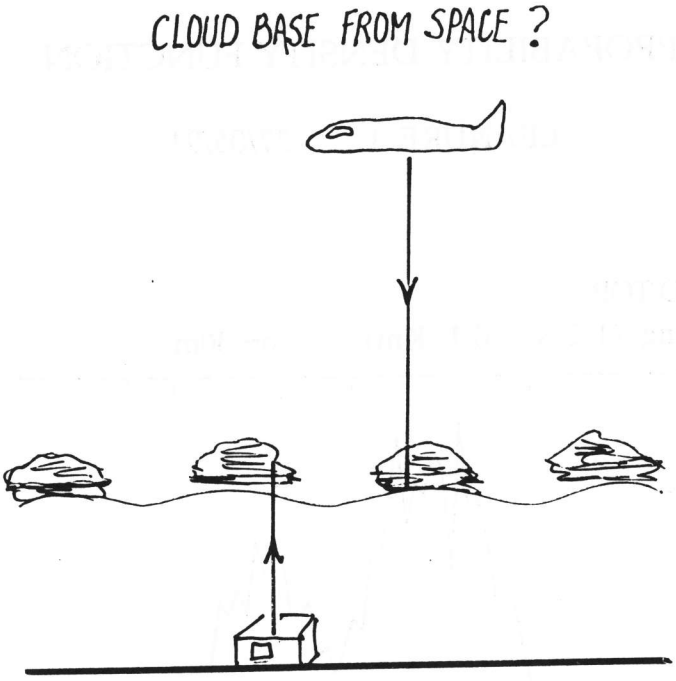

Base & top of cumulus clouds.

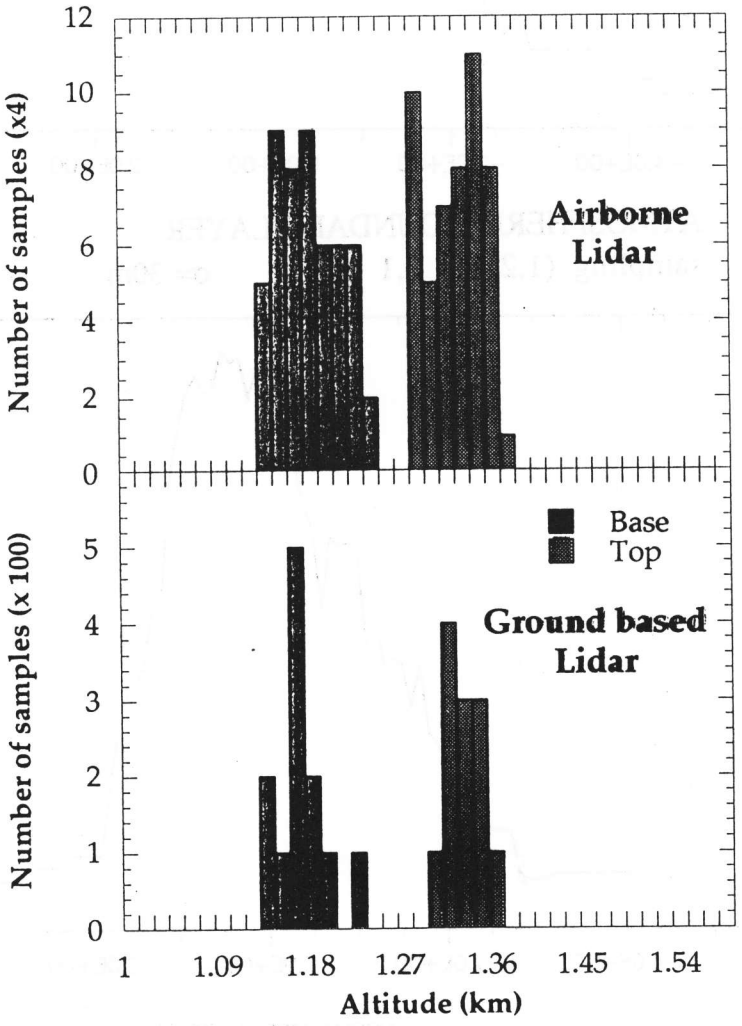

SYNERGY BETWEEN ACTIVE AND PASSIVE REMOTE SENSORS

INFRARED RADIOMETER

POLDER

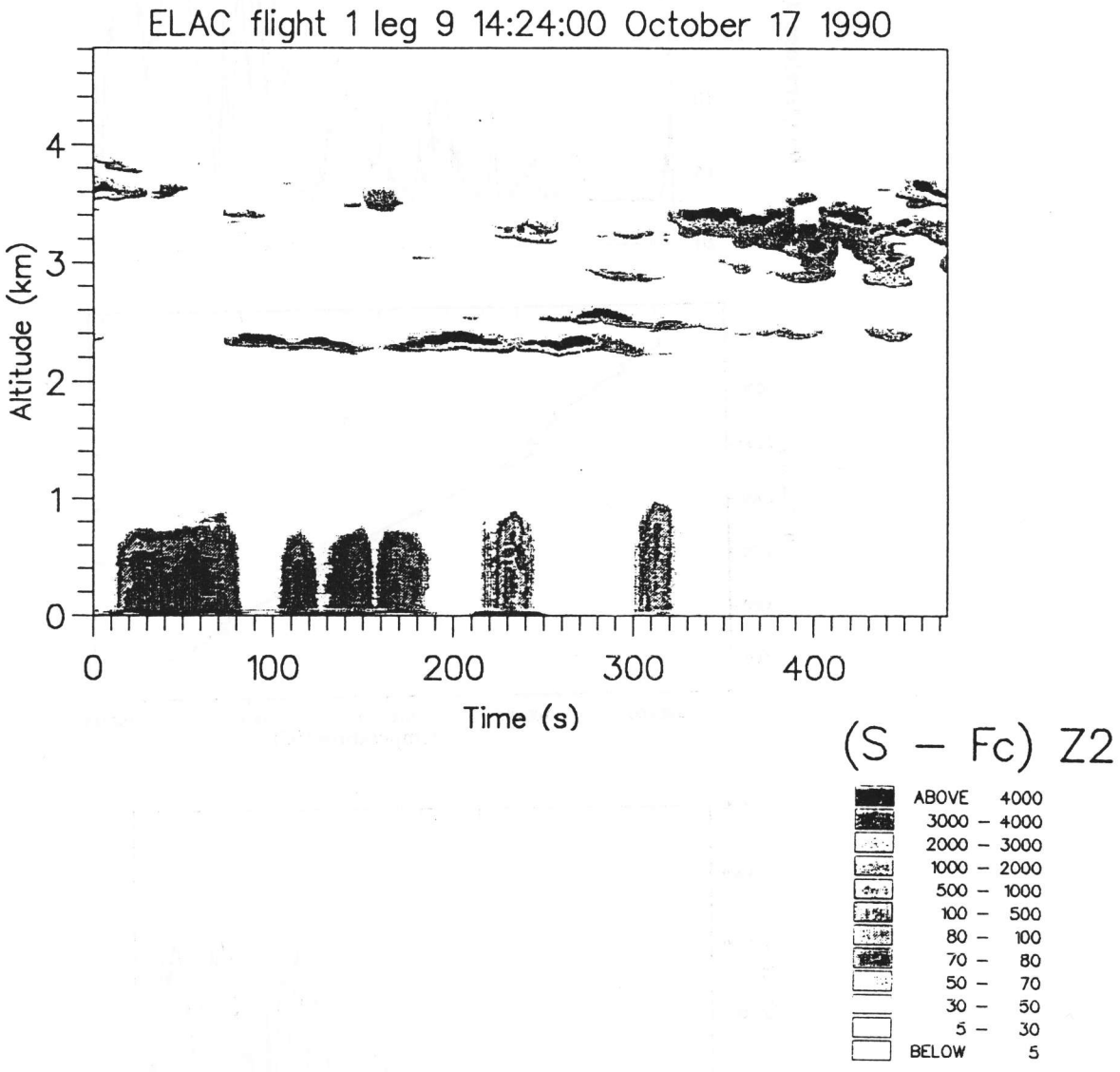

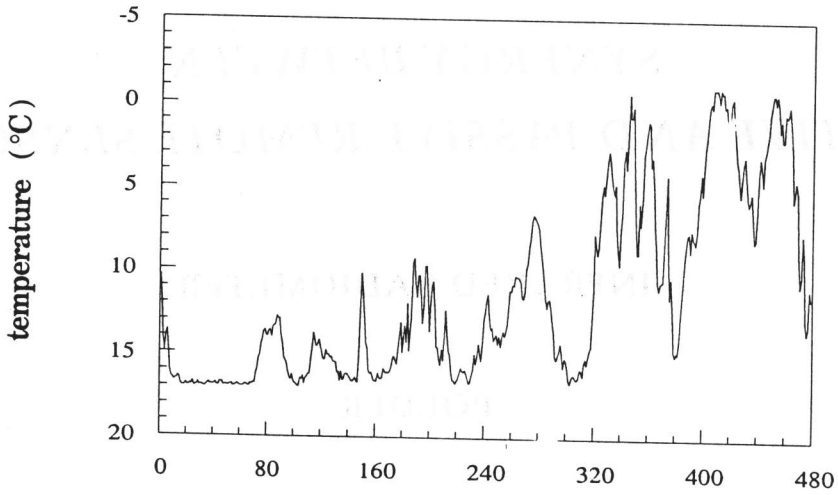
temperature (°C)
-5
0
5
10
15
20
0
80
160
240
320
400
480

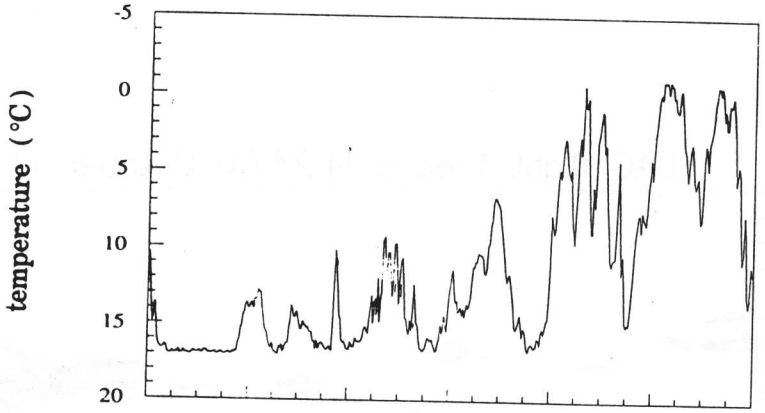
temperature (°C)
-5
0
5
10
15
20

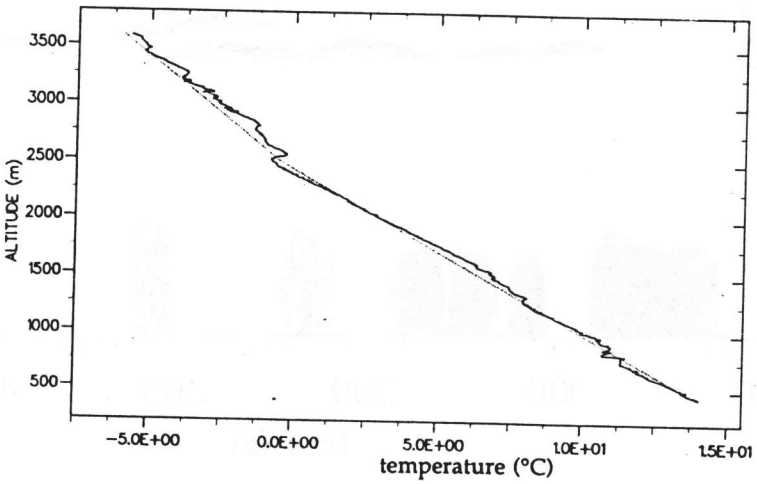
ALTITUDE (m)
3500
3000
2500
2000
1500
1000
500
-5.0E+00
0.0E+00
5.0E+00
1.0E+01
1.5E+01
temperature (°C)

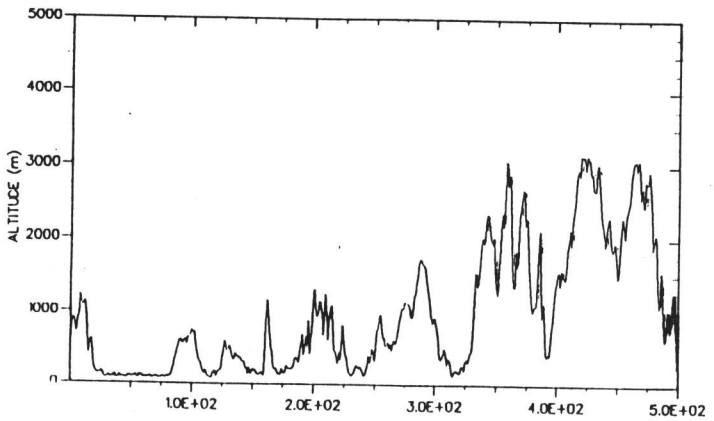
ALTITUDE (m)
5000
4000
3000
2000
1000
0
1.0E+02
2.0E+02
3.0E+02
4.0E+02
5.0E+02

EUCREX'94 :

European Cloud Radiation Experiment

FALCON (above the cloud) :

- Microphysical measurements
- POLDER downward viewing
- Fluxes SW and LW

ARAT (below the cloud):

- Lidar upward viewing (0.55 µm)
- Radiometer upward (9.5 -11.5 µm)
- Fluxes SW and LW

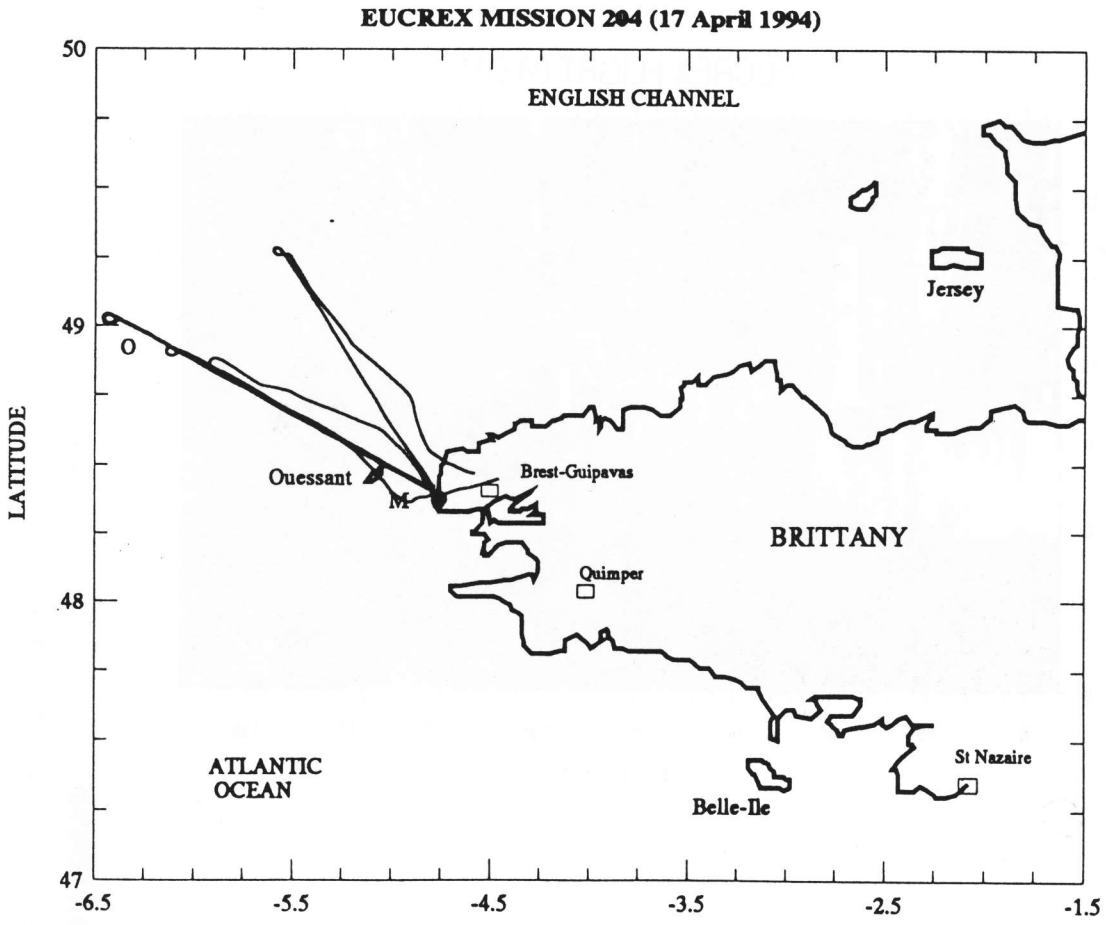

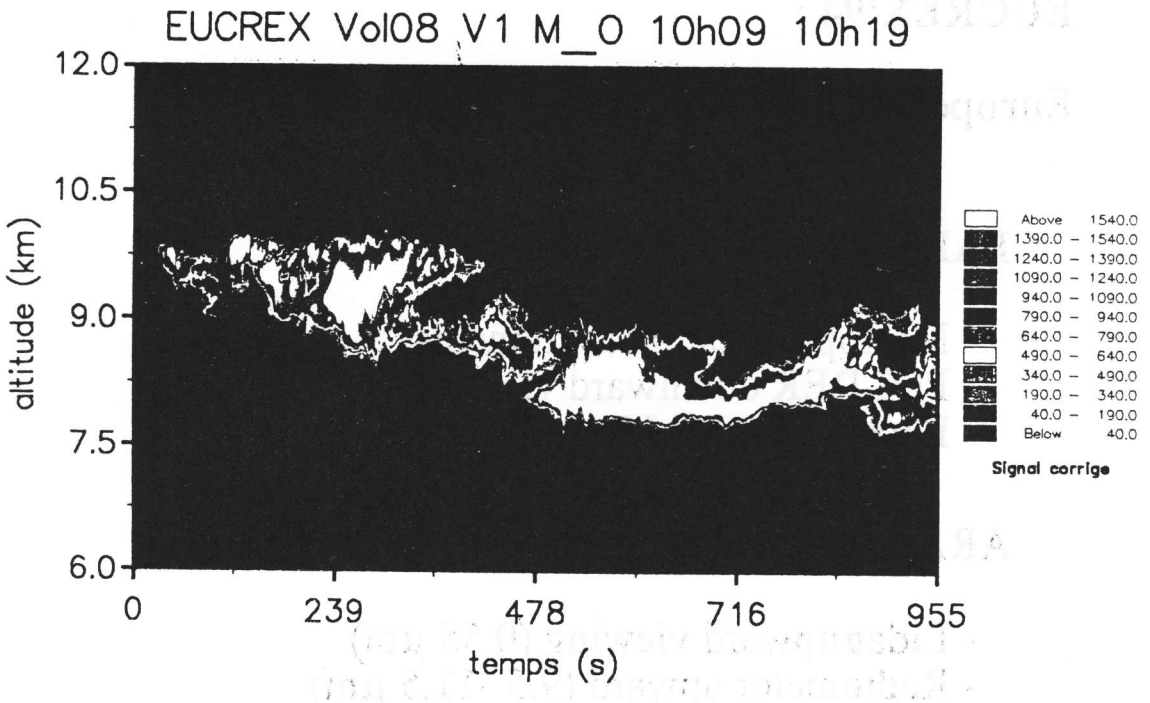
EUCREX Vol08 V1 M_O 10h09 10h19
altitude (km)
12.0
10.5
9.0
7.5
6.0
0
239
478
716
955
temps (s)
Above 1540.0
1390.0 - 1540.0
1240.0 - 1390.0
1090.0 - 1240.0
940.0 - 1090.0
790.0 - 940.0
640.0 - 790.0
490.0 - 640.0
340.0 - 490.0
190.0 - 340.0
40.0 - 190.0
Below 40.0
Signal corrige

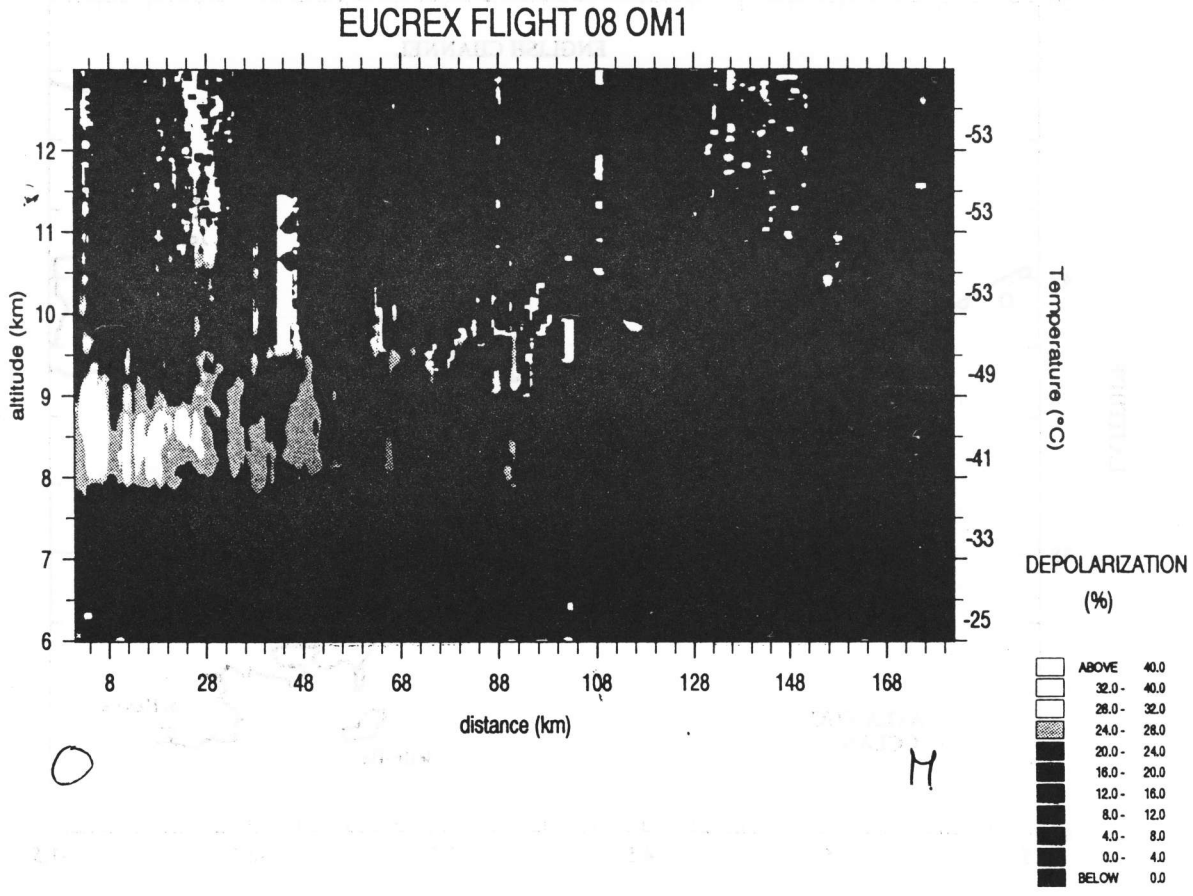
EUCREX FLIGHT 08 OM1
altitude (km)
12
11
10
9
8
7
6
8
28
48
68
88
108
128
148
168
distance (km)
-53
-53
-53
-49
-41
-33
-25
Temperature (°C)
DEPOLARIZATION
(%)
ABOVE 40.0
32.0 - 40.0
28.0 - 32.0
24.0 - 28.0
20.0 - 24.0
16.0 - 20.0
12.0 - 16.0
8.0 - 12.0
4.0 - 8.0
0.0 - 4.0
BELOW 0.0

DEPOLARIZATION

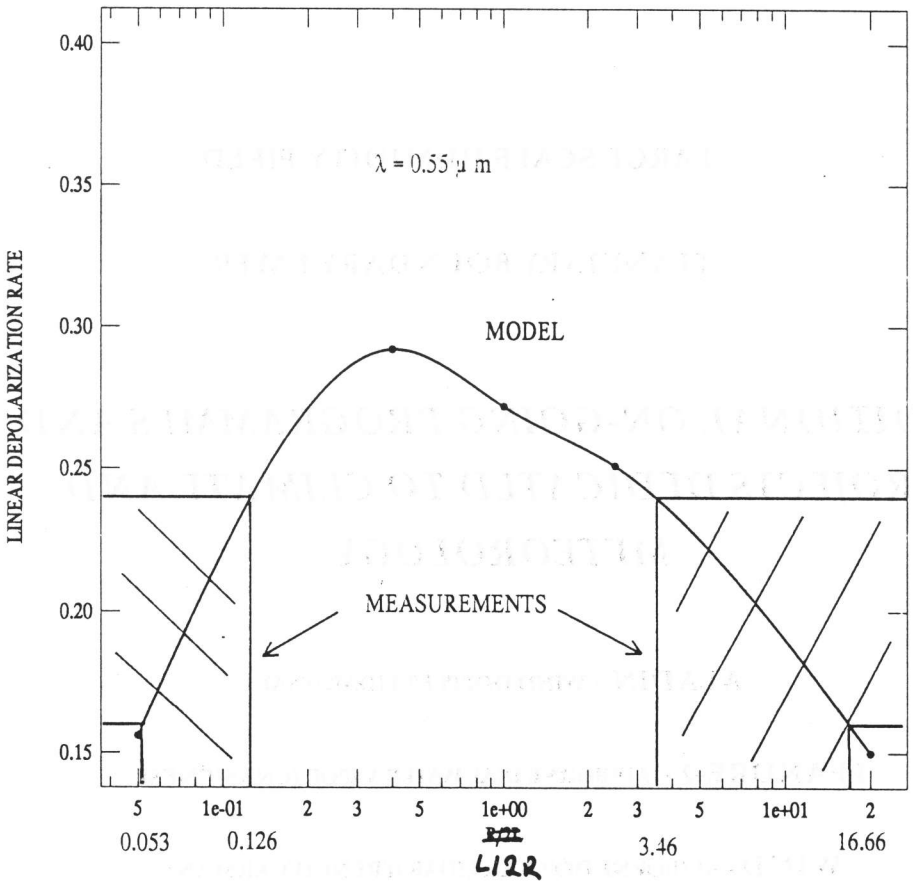

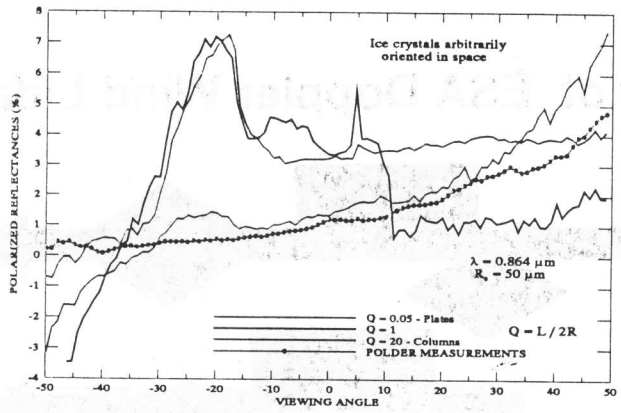

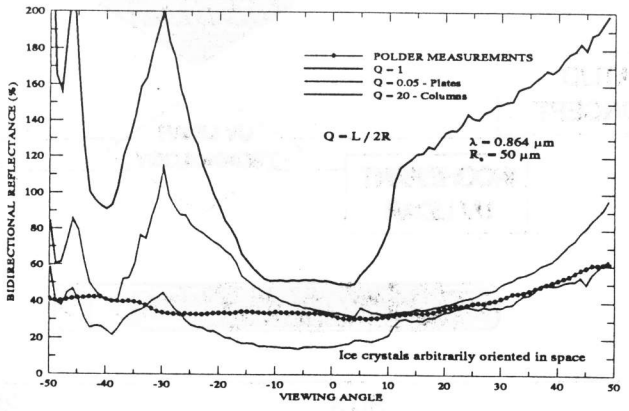

COMPARISONS IN THE SOLAR PRINCIPAL PLANE

SPACE BASED DIAL-WATER VAPOR LIDAR

LARGE SCALE HUMIDITY FIELD

PLANETARY BOUNDARY LAYER

ADDITIONAL ON-GOING PROGRAMMES AND PROJECTS DEDICATED TO CLIMATE AND METEOROLOGY

ALADIN - WIND DOPPLER LIDAR (ESA)

LEANDRE-2 - AIRBORNE DIAL WATER VAPOR (CNRS/CNES)

WIND - AIRBORNE DOPPLER LIDAR (FRENCH/GERMAN)